IEEE Access
Multidisciplinary | Rapid Review | Open Access Journal

Received March 19, 2018, accepted April 19, 2018, date of publication May 4, 2018, date of current version May 24, 2018.

Digital Object Identifier 10.1109/ACCESS.2018.2832616

Blind System Identification Using Symbolic Dynamics

SUMONA MUKHOPADHYAY AND HENRY LEUNG, (Fellow, IEEE)
Department of Electrical and Computer Engineering, University of Calgary, Calgary, AB T2N 1N4, Canada
Corresponding author: Sumona Mukhopadhyay (mukhopas@ucalgary.ca)

ABSTRACT In this paper, a chaos-based approach is proposed for system identification with binary random signal. A chaos-based approach is developed to model random binary sequence and is applied to blind system identification. The Cramér Rao Lower Bound (CRLB)-based on the chaos representation is derived. The theoretical mean square error of the proposed approach is also derived. It is shown that the proposed blind approach achieves the CRLB asymptotically. The proposed technique is applied to blind channel equalization of a quadrature amplitude modulation communication system. The equalizer is based on expected maximization and unscented Kalman filtering and smoother. Our proposed method shows superior performance in comparison with conventional blind equalization techniques. The significance of this research is to extend the advantages of chaos to random signals for the blind system identification.

INDEX TERMS Chaos, binary symbols, blind, equalization, Cramér Rao lower bound, expectation maximization, quadrature amplitude modulation, symbolic dynamics, system identification, unscented Kalman filter.

I. INTRODUCTION

The properties of chaotic signals such as broadband spectra, aperiodicity and sensitivity to initial conditions have been a catalyst in the growth of research concerning application of chaos to signal processing [1]–[3], communications [4]–[7] and other engineering applications [8]–[16]. There are two main approaches of employing chaos in signal processing. The first approach applies chaos to model natural signals such as speech, radar clutter, and biomedical signals. The other approach is to generate the chaotic signals and to employ their unique chaotic properties to enhance system performance such as system identification. In signal processing, previous studies have proved that employing chaos provides superior performance in blind system identification as compared to random signals [17], [18]. But applying chaos has few challenges besides having numerous merits.

The first challenge lies in the estimation of chaotic signals. These signals appear to be noise-like and can be analyzed and processed using techniques for stochastic signals. However, chaotic signals contain more information that cannot be inferred from and exploited by traditional stochastic modeling techniques. As such many studies have been dedicated to design robust and efficient algorithms for estimating chaotic signals in the presence of noise. One such method is the dynamic estimation method based on itinerary [19]–[23]. However, these techniques are not suitable for real time estimation due to the highly irregular nature of the cost function. Despite being asymptotically efficient at high signal-to-noise ratio (SNR), these methods have suboptimal performance. Maximum Likelihood (ML) method with Viterbi search [24], [25] and its enhanced versions [26], [27] have also been developed. Although these approaches suffer from heavy computational load and suboptimal performance, their results indicate that symbolic dynamics is resistant to noise [23]. Moreover, symbolic dynamics based modulation has also been useful in improving synchronization performance in spread spectrum communications [28]. Therefore, symbolic dynamics has great potential in signal processing.

Another challenge in applying chaos to signal processing is to ensure that the received signal is indeed chaotic after it is corrupted by noise. It is not easy to distinguish whether the aperiodicity is due to the random nature of the chaotic waveform or due to noise [29]. Moreover, it is challenging to ensure that the received signal does not cease to be chaotic due to the lack of sensitive dependence on initial conditions in noisy environments [30].

Finally, in transmitting a chaotic signal, the received signal may not match the chaotic map which results in large errors. Therefore, many chaos-based applications could not show any significant improvement compared to the conventional

approaches. In chaos-based communications, various techniques [31]–[33] have been proposed but they performed well only at moderate noise levels. State-space approaches are also designed by linearizing of the chaotic map [34]–[37]. However, such a linearizing approach does not fully exploit the nonlinear dynamics.

We can infer that the aforementioned problems arise due to the stringent requirement of transmitting a chaotic signal which restricts the benefits of using chaos. This raises a pertinent question which is: "Is there a way to exploit the potential of chaos in applications that does not mandate the requirement of the transmitted signal to be chaotic?" Using the fact that a random dynamical system can be represented by chaos [38], we propose to apply chaos to represent a random symbolic signal (RS) for signal processing. Such an approach can be of great interest to the current big data era where data are categorial variables and many data analytic methods hash data to binary symbolic format.

In this work, we use system identification to illustrate how chaos can be used to improve blind system identification using binary valued RS signal. In our work, the chaos representation of RS is not restricted to only binary symbolic sequence. This technique can be applied to blind equalization when the transmitted signal is a multi-level RS. Our motivation of using chaos comes from our previous results [17], [18] where it is proved that chaos has the potential of improving blind system identification in signal processing. However, it is based on a strong assumption that the signal should be chaotic. In real life, it is difficult for signals to follow the strict definition of chaos. In order to reap the benefits of chaos in signal processing, a new angle of using chaos is proposed by using chaotic representation to model RS using the concept of symbolic dynamics. The advantage of using symbolic dynamics to model RS is that it allows the chaotic properties such as the Lyapunov Exponent (LE) to be preserved. In other words, by applying symbolic dynamics, an equivalent chaotic dynamical system which is known as the chaotic shift map [39] is obtained which allows any random symbolic sequence to be generated from chaotic dynamics.

In this work, the LE of the chaotic map and the deterministic property of chaos are exploited to improve blind system identification performance when RS is the input to the system. The Expectation Maximization and Unscented Kalman Smoother (EM-UKS) [18], [40] algorithm for system identification starts from randomly generating the RS sequence. The main difference between the way EM-UKS is applied in this work compared to those in [18] and [40] is that the estimation algorithm uses the chaotic representation scheme of the RS and the conjugacy relations. Due to the deterministic property of chaotic maps, the estimation of the initial value x_0 with which the chaotic map is iterated to produce the chaotic symbolic signal is equivalent to estimating the whole signal. Using this proposed method, the chaotic map which is used to model the RS is assumed to be known. However, we also show that blind system identification can be performed by approximating the unknown nonlinear chaotic map using predictors constructed by some nonlinear function approximators [41]. In this paper, the system or channel to be identified is a Moving Average (MA) model. The RS sequence is used to excite the system so that the system can be identified from the output signal. The question we try to answer is: "Could chaos be applied to process general random symbolic signals so that the advantage of chaos in system identification can be extended to blind system identification using RS?"

The contributions and novelty of our work are summarized as follows:

- Blind system identification is formulated using chaos representation of RS.
- The Cramér Rao Lower Bound (CRLB) for chaos representation of RS is derived.
- The theoretical mean square error (MSE) performance is derived.
- The proposed approach is used in blind channel equalization in a QAM system.

The paper is organized as follows: In Section II, the formulation of the blind system identification problem is given. Section III presents the proposed methodology. In Section IV the CRLB and the MSE using chaos is derived. In Section V, the blind identification method based on Expectation Maximization Unscented Kalman Smoother (EM-UKS) is developed. Performance evaluation of blind system identification with application to communications are discussed in Section VI. Concluding remarks are given in Section VII.

Notation: $\mathbb{C}$ and $\mathbb{R}$ denote the sets of complex and real numbers, respectively. The real and imaginary parts of a complex number are denoted by $\mathrm{Re}(\cdot)$ and $\mathrm{Im}(\cdot)$ respectively. All vectors and matrices are given in *bold*, with lower case letters representing vectors, and upper case letters representing matrices. Scalars are given in normal type. $\mathcal{CN}$ represents circularly symmetric Gaussian distribution. The symbols $(\cdot)^{\mathsf{T}}$, $(\cdot)^*$, $(\cdot)^{\mathsf{H}}$, and $E[\cdot]$ signify the transpose of a matrix, the conjugate, the conjugate transpose and the expectation operator, respectively.

II. PROBLEM FORMULATION

Let, $\mathbf{s} = \{s_1, s_2, \ldots, s_n, \ldots, s_N\}$ be the input RS, independently and identically distributed (i.i.d). Each s_n is a source symbol characterized by equal probability and takes value from a finite alphabet set $s_n \in \mathbb{A} = \{a_1, \ldots, a_M\}$, where a_k are real or complex numbers. The output of the system is corrupted by a zero mean Additive White Gaussian noise (AWGN) $v \sim \mathcal{CN}(0, 2\sigma_v^2)$ having variance σ_v^2. Thus, the received noisy signal $y_n \in \mathbb{C}$ is expressed as:

$$y_n = \mathbf{h}^{\mathsf{H}}\mathbf{s}_n + v_n. \tag{1}$$

$\mathbf{h} = [h_0, h_1, \ldots, h_{L-1}]^{\mathsf{T}} \in \mathbb{C}^{L\times 1}$ of length L which represents the coefficients of the system, and $\mathbf{s}_n = [s_n, s_{n-1}, s_{n-2}, \ldots, s_{n-L+1}]^{\mathsf{T}}$ having a variance of σ^2. Blind system identification problem using chaos is to estimate

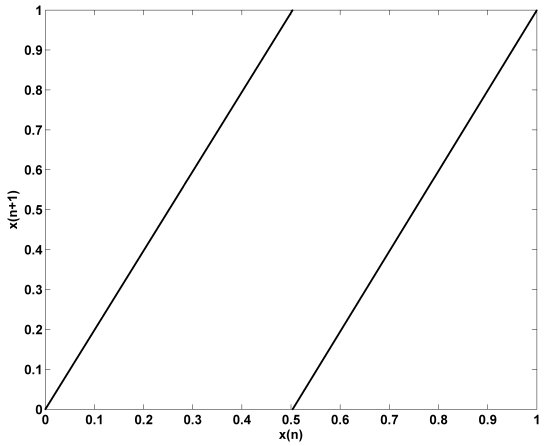

FIGURE 1. Plot of PWL for m = 2 symbols.

$\theta^* = \{\mathbf{h}, x_0, \sigma_v^2\} \in \mathbb{C}$ from the noisy measurement signal vector, $\mathbf{y} = [y_0, y_1, \ldots, y_{N-1}]$ only where x_0 is the initial condition of the chaotic map f.

III. METHODOLOGY: CHAOS REPRESENTATION OF RANDOM SYMBOLIC SEQUENCE

In our work, the chaotic modeling strategy of the RS begins by the inverse interval mapping method. To model a RS using a chaotic map, the one-to-one correspondence between the initial point and its symbolic itinerary (sequence) is applied [42]. When the RS contains only two distinct symbols $\{\pm 1\}$, the piecewise linear (PWL) chaotic map has two disjoint linear segments which is obtained by adjusting to the symbol probability p of the binary-valued RS as shown in Fig. 1. By knowing the value of the symbol at s_n, x_n can be determined by the reverse interval mapping method given by:

$$x_n = f_{s_n}^{-1}(x_{n+1}), \tag{2}$$

where $f_{s_n}^{-1}$ is the pre-image of the chaotic signal for an appropriate branch of $f_{s_n}^{-1}$ given by:

$$f_{s_n}^{-1}(x_{n+1}) = \begin{cases} p \times x_{n+1}, & \text{for symbol } s_n = a_1 \\ p + (1-p) \times x_{n+1}, & \text{for symbol } s_n = a_2 \end{cases} \tag{3}$$

and the PWL chaotic map f is defined as follows:

$$x_{n+1} = f(x_n) = \begin{cases} x_n/p, & \text{for } x_n \in I_{a_1} \\ (x_n - p)/(1-p) & \text{for } x_n \in I_{a_2} \end{cases} \tag{4}$$

where the intervals I_{a_1}, I_{a_2} denotes the interval for the symbol $a_1 = -1$ and $a_2 = +1$ respectively. By the recursive application of the inverse function mapping, the initial condition can be obtained. The symbolic sequence itinerary is then obtained from,

$$s_{n+1} = \Theta(f^n(x_0)) = \Theta(x_{n+1}). \tag{5}$$

where $\Theta(\cdot)$ is expressed as:

$$s_n = \Theta(x_n) = \begin{cases} -1 & \text{if } x_n \in I_{a_1} \\ +1, & \text{if } x_n \in I_{a_2} \end{cases} \tag{6}$$

By using $\Theta(\cdot)$, a corresponding chaotic dynamical system $\sigma(.)$ which is known as the chaotic shift map is created. $\sigma(.)$ generates chaotic symbolic signal (CS) which is related to the chaotic map f via Θ by the relation:

$$\sigma(s) = \Theta(f(\Theta^{-1}(s))). \tag{7}$$

The chaotic map $\sigma(\cdot)$ is conjugate to the chaotic map $f(\cdot)$ via $\Theta(\cdot)$ where $\Theta(\cdot)$ acts as a mapping function between the chaotic dynamics and the symbolic dynamics. The dynamics governing the symbolic sequence is represented by a left shift operation where the leftmost symbol is discarded at each iteration, shown as follows:

$$\mathbf{s}_n = \sigma(s_n s_{n+1} \ldots) = s_{n+1} s_{n+2} \ldots. \tag{8}$$

This means that any itinerary-based algorithm for estimating initial points for the map f will give rise to a corresponding itinerary-based algorithm for the map σ [20]. Hence, $\mathbf{x} = \{x_1, x_2, \ldots, x_n, \ldots, x_N\}$ can be represented as a string $\mathbf{s} = \{s_1, s_2, \ldots s_n, \ldots, s_N\}$ obtained from (8). The chaos representation of RS for the proposed system identification method is expressed as:

$$\begin{aligned} z_n &= \mathbf{h}^{\mathsf{H}} \Theta(\mathbf{f}^{n-1}(\mathbf{f}_{\mathbf{s}_n}^{-(N-1)}(\alpha))), \\ &= \mathbf{h}^{\mathsf{H}} \Theta(\mathbf{f}^{n-1}(\mathbf{x}_0)), \\ &= \mathbf{h}^{\mathsf{H}} \sigma(\mathbf{s}_{n-1}), \\ &= \mathbf{h}^{\mathsf{H}} \mathbf{s}_n. \end{aligned} \tag{9}$$

α is a point in the interval I and the use of reverse interval mapping is guided by the symbolic sequence which can converge towards an initial condition x_0 as shown below:

$$x_0 = f_{s_0}^{-1}(x_1) = f_{s_0 s_1}^{-1}(x_2) = \ldots = f_{s_0,\ldots,s_{N-1}}^{-1}(x_N). \tag{10}$$

In this way, an RS can be treated as being generated from CS.

IV. THEORETICAL PERFORMANCE ASSESSMENT

In this section, we derive the CRLB of blind system identification using the RS representation of chaos. The CRLB is defined as:

$$var(\hat{\theta}) \geq \mathbf{J}^{-1}(\theta), \tag{11}$$

where $\mathbf{J}(\theta)$ is the complex Fisher Information Matrix (FIM) expressed as:

$$[\mathbf{J}(\theta)] = -E\left[\frac{\partial \ln \mathsf{P}(\mathbf{y}|\theta)}{\partial \theta}\left(\frac{\partial \ln \mathsf{P}(\mathbf{y}|\theta)}{\partial \theta}\right)^{\mathsf{H}}\right]. \tag{12}$$

The derivation is based on employing the conjugate relationship given in (7) which means that $\Theta(\cdot)$ converts the orbits of x_0 under $f(\cdot)$ to orbits of $\Theta(x_0)$ under $\sigma(.)$ i.e., $x_0, f(x_0), f^2(x_0), f^3(x_0), \ldots, f^n(x_0)$ to $\Theta(x_0)$, $\sigma(\Theta(x_0))$, $\sigma^2(\Theta(x_0))$, $\sigma^3(\Theta(x_0)), \ldots, \sigma^n(\Theta(x_0))$. So, the

symbols $(s_1, s_2, \ldots)$ are the output of the chaotic dynamical shift map $\sigma(\cdot)$. Hence, there is an equivalence relation between the two chaotic dynamical systems, $f(\cdot) \Longleftrightarrow \sigma(\cdot)$. This connection between chaotic numeric and its symbols is used to derive the CRLB as follows. From (9) the likelihood is given by:

$$\mathsf{P}(\mathbf{y}|\theta) = \prod_{n=0}^{N-1} \frac{1}{2\pi\sigma_v^2} \exp\left(\frac{-(y_n - z_n)^{\mathsf{H}}(y_n - z_n)}{2\sigma_v^2}\right) \tag{13}$$

The log–likelihood expression is:

$$\begin{aligned}\ell(\mathbf{y}|\theta) = & -N\ln(2\pi) - 2N\ln\sigma_v \\ & -\frac{1}{2\sigma_v^2}\left[\sum_{n=0}^{N-1}(y_n - \mathbf{h}^{\mathsf{H}}\mathbf{s}_n)^{\mathsf{H}}(y_n - \mathbf{h}^{\mathsf{H}}\mathbf{s}_n)\right]\end{aligned} \tag{14}$$

The complex gradient $\frac{\partial \ell(\mathbf{y}|\theta^*)}{\partial \theta^*}$ for the complex parameter vector θ^* is related to the real gradient $\frac{\partial \ln p}{\partial \operatorname{Re}\theta}$ by the relation:

$$\begin{aligned}\frac{\partial \ln p}{\partial \theta^*} &= \begin{bmatrix} \frac{\partial \ell(\mathbf{y}|\theta)}{\partial \mathbf{h}^*} \\ \frac{\partial \ell(\mathbf{y}|\theta)}{\partial \mathbf{h}} \\ \frac{\partial \ell(\mathbf{y}|\theta)}{\partial x_0^*} \\ \frac{\partial \ell(\mathbf{y}|\theta)}{\partial x_0} \\ \frac{\partial \ell(\mathbf{y}|\theta)}{\partial \sigma_v^2} \end{bmatrix} = \begin{bmatrix} \frac{1}{2} & \frac{j}{2} & 0 & 0 & 0 \\ \frac{1}{2} & \frac{-j}{2} & 0 & 0 & 0 \\ 0 & 0 & \frac{1}{2} & \frac{j}{2} & 0 \\ 0 & 0 & \frac{1}{2} & \frac{-j}{2} & 0 \\ 0 & 0 & 0 & 0 & 1 \end{bmatrix} \begin{bmatrix} \frac{\partial \ell(\mathbf{y}|\theta)}{\partial \operatorname{Re}\mathbf{h}} \\ \frac{\partial \ell(\mathbf{y}|\theta)}{\partial \operatorname{Im}\mathbf{h}} \\ \frac{\partial \ell(\mathbf{y}|\theta)}{\partial \operatorname{Re} x_0} \\ \frac{\partial \ell(\mathbf{y}|\theta)}{\partial \operatorname{Im} x_0} \\ \frac{\partial \ell(\mathbf{y}|\theta)}{\partial \sigma_v^2} \end{bmatrix} \\ &= \mathbf{T}\frac{\partial \ell(\mathbf{y}|\theta)}{\partial \operatorname{Re}\theta}\end{aligned} \tag{15}$$

The complex CRLB of the complex parameter vector can then be connected to the CRLB of the real number as [43], [44]:

$$\mathrm{CRLB}(\theta^*) = [\mathbf{T}^{\mathsf{H}}]^{-1}\mathrm{CRLB}(\operatorname{Re}\theta)\mathbf{T}^{-1} \tag{16}$$

Therefore, we can derive the CRLB in terms of the real valued parameter vector $\operatorname{Re}\theta = \{\operatorname{Re}\mathbf{h}, \operatorname{Im}\mathbf{h}, \operatorname{Re}x_0, \operatorname{Im}x_0, \sigma_v^2\}$. The details of the derivation are presented in the Appendix. The CRLB using the chaotic representation of RS denoted by $CRLB_{enc}^{(B)}$ is expressed as:

$$\begin{aligned}CRLB_{enc}^{(B)} &= 2\sigma_v^2 tr\Big(\sum_{n=0}^{N-1} E[\mathbf{s}_n\mathbf{s}_n^{\mathsf{H}}]^{-1}\Big) \\ &= \frac{2\sigma_v^2}{N} tr\left(\left[E[\mathbf{s}_n\mathbf{s}_n^{\mathsf{H}}]\right]^{-1}\right)\end{aligned} \tag{17}$$

In [18], it is found that for a Moving Average (MA) model, the CRLB of non-blind system identification using RS (denoted as $CRLB_{RS}^{(NB)}$) is similar to the CRLB of blind system identification when the driving signal is a CS signal (denoted as $CRLB_{CS}^{(B)}$), i.e.,

$$\begin{aligned}CRLB_{RS}^{(NB)} &= CRLB_{CS}^{(B)} \\ &= \sigma_v^2 tr\left(\left[\sum_{n=1}^{N} E[\mathbf{s}_n\mathbf{s}_n^{\mathsf{T}}]\right]^{-1}\right).\end{aligned} \tag{18}$$

From (17) and (18), we observe that for an MA model,

$$CRLB_{enc}^{(B)} = CRLB_{RS}^{(NB)} = CRLB_{CS}^{(B)}. \tag{19}$$

To understand the effectiveness of the proposed method, the theoretical MSE performance of the estimated parameters is derived and compared with the the CRLB. Using (7) and (8) we have,

$$\Theta(x_{n+1}) = \sigma(s_n) = s_{n+1}. \tag{20}$$

This expression means that the symbols $(s_1, s_2, \ldots)$ are the outputs of the chaotic shift map $\sigma(\cdot)$. We can re-express the formulation in terms of the chaotic map $\sigma(\cdot)$:

$$s_{n+1} = \sigma(s_n). \tag{21}$$

which defines the dynamical system in the symbol-space representation. The estimates $\operatorname{Re}\hat{\mathbf{h}}$, $\operatorname{Im}\hat{\mathbf{h}}$, $\operatorname{Re}\hat{x_0}$, $\operatorname{Im}\hat{x_0}$, $\hat{\sigma_v^2}$ are obtained from equating the first order derivative of the log–likelihood expression in (14) to zero, i.e.,

$$\frac{\partial \ell(\mathbf{y}|\theta)}{\partial \mathbf{h}} = \frac{1}{\sigma_v^2}\sum_{n=0}^{N-1}(y_n - \hat{\mathbf{h}}^{\mathsf{H}}\hat{\mathbf{s}}_n)\hat{\mathbf{s}}_n^{\mathsf{H}} = 0, \tag{22}$$

Replacing y_n in (22),

$$\begin{aligned}&\sum_{n=1}^{N}\left[(\mathbf{h}^{\mathsf{H}}\mathbf{s}_n + v_n - \hat{\mathbf{h}}^{\mathsf{H}}\hat{\mathbf{s}}_n)\hat{\mathbf{s}}_n^{\mathsf{H}}\right] = 0, \\ &\sum_{n=1}^{N}\left[(\hat{\mathbf{h}}^{\mathsf{H}}\hat{\mathbf{s}}_n - \mathbf{h}^{\mathsf{H}}\mathbf{s}_n - v_n)\hat{\mathbf{s}}_n^{\mathsf{H}}\right] = 0, \\ &\sum_{n=1}^{N}\left[\hat{\mathbf{h}}^{\mathsf{H}}\hat{\mathbf{s}}_n\hat{\mathbf{s}}_n^{\mathsf{H}} - \mathbf{h}^{\mathsf{H}}\mathbf{s}_n\hat{\mathbf{s}}_n^{\mathsf{H}} - v_n\hat{\mathbf{s}}_n^{\mathsf{H}}\right] = 0, \\ &\hat{\mathbf{h}}^{\mathsf{H}}\Big[\sum_{n=1}^{N}\hat{\mathbf{s}}_n\hat{\mathbf{s}}_n^{\mathsf{H}}\Big] = \sum_{n=1}^{N}\left[v_n\hat{\mathbf{s}}_n^{\mathsf{H}} + \mathbf{h}^{\mathsf{H}}\mathbf{s}_n\hat{\mathbf{s}}_n^{\mathsf{H}}\right], \\ &(\hat{\mathbf{h}}^{\mathsf{H}} - \mathbf{h}^{\mathsf{H}})\sum_{n=1}^{N}\mathbf{s}_n\mathbf{s}_n^{\mathsf{H}} - \sum_{n=1}^{N}v_n\hat{\mathbf{s}}_n^{\mathsf{H}} = 0, \\ &\Delta\mathbf{h}^{\mathsf{H}}\sum_{n=1}^{N}\hat{\mathbf{s}}_n\hat{\mathbf{s}}_n^{\mathsf{H}} = \sum_{n=1}^{N}v_n\hat{\mathbf{s}}_n^{\mathsf{H}}, \\ &\Delta\mathbf{h}^{\mathsf{H}} = \Big(\sum_{n=1}^{N}v_n\hat{\mathbf{s}}_n^{\mathsf{H}}\Big)\Big[\sum_{n=1}^{N}\hat{\mathbf{s}}_n\hat{\mathbf{s}}_n^{\mathsf{H}}\Big]^{-1}, \\ &\Delta\mathbf{h} = \Big(\sum_{n=1}^{N}v_n\hat{\mathbf{s}}_n^{\mathsf{H}}\Big)^{\mathsf{H}}\left(\left[\sum_{n=1}^{N}\hat{\mathbf{s}}_n\hat{\mathbf{s}}_n^{\mathsf{H}}\right]^{-1}\right)^{\mathsf{H}}.\end{aligned} \tag{23}$$

Since the input is zero mean, so $E[\sum_{n=1}^{N}\hat{\mathbf{s}}_n\hat{\mathbf{s}}_n^{\mathsf{H}}] = \sigma^2$. Next, in order to distinguish between $\Delta\mathbf{h}^{\mathsf{H}}$ and $\Delta\mathbf{h}$, we now use the symbol dash ($'$) in the subscript of variables to denote the terms for $\Delta\mathbf{h}^{\mathsf{H}}$ and the un-dashed variables denote the terms

for $\Delta\mathbf{h}$. The corresponding MSE of the coefficients denoted as MSE_h can be derived as:

$$E\left[\Delta\mathbf{h}^{\mathsf{H}}\Delta\mathbf{h}\right] = tr\Bigg(E\Bigg[\Bigg(\sum_{n=1}^{N} v_n\hat{\mathbf{s}}_n^{\mathsf{H}}\Bigg)\times\Bigg(\sum_{n'=1}^{N} v_{n'}\hat{\mathbf{s}}_{n'}^{\mathsf{H}}\Bigg)^{\mathsf{H}} \times\Bigg(\sum_{n=1}^{N}\hat{\mathbf{s}}_n\hat{\mathbf{s}}_n^{\mathsf{H}}\Bigg)^{-1}\times\Bigg(\sum_{n'=1}^{N}\hat{\mathbf{s}}_{n'}\hat{\mathbf{s}}_{n'}^{\mathsf{H}}\Bigg)^{-\mathsf{H}}\Bigg]\Bigg),$$
$$= tr\Bigg(\sum_{n'=1}^{N}\sum_{n=1}^{N}E\left[v_n v_{n'}^{\mathsf{H}}\right]\times\sum_{n'=1}^{N}\sum_{n=1}^{N}\left[E\left[\hat{\mathbf{s}}_n\hat{\mathbf{s}}_{n'}^{\mathsf{H}}\right]\right]^{\mathsf{H}} \times\sum_{n=1}^{N}\left[E\left[\hat{\mathbf{s}}_n\hat{\mathbf{s}}_n^{\mathsf{H}}\right]\right]^{-1}\times\sum_{n'=1}^{N}\left[E\left[\hat{\mathbf{s}}_{n'}\hat{\mathbf{s}}_{n'}^{\mathsf{H}}\right]\right]^{-\mathsf{H}}\Bigg). \tag{24}$$

Using $\sum_{n'=1}^{N}\sum_{n=1}^{N} v_n v_n^{\mathsf{H}} = 2N\sigma_v^2$, we have:

$$E\left[\Delta\mathbf{h}^{\mathsf{H}}\Delta\mathbf{h}\right] = 2tr\Bigg(N\sigma_v^2\sum_{n=1}^{N}\left[E\left[\hat{\mathbf{s}}_n\hat{\mathbf{s}}_n^{\mathsf{H}}\right]\right]^{\mathsf{H}} \times\sum_{n=1}^{N}\left[E[\hat{\mathbf{s}}_n\hat{\mathbf{s}}_n^{\mathsf{H}}]\right]^{-1}\times\sum_{n=1}^{N}\left[E\left[\hat{\mathbf{s}}_n\hat{\mathbf{s}}_n^{\mathsf{H}}\right]\right]^{-\mathsf{H}}\Bigg), \tag{25}$$

$$= 2N\sigma_v^2 tr\Bigg(\Bigg[E[\sum_{n=1}^{N}\hat{\mathbf{s}}_n\hat{\mathbf{s}}_n^{\mathsf{H}}]\Bigg]^{-1}\Bigg),$$
$$= 2N\sigma_v^2\frac{1}{N}tr\Bigg(\Bigg[E[\hat{\mathbf{s}}_n\hat{\mathbf{s}}_n^{\mathsf{H}}]\Bigg]^{-1}\Bigg),$$
$$= 2\sigma_v^2 tr\Bigg(\Bigg[E[\hat{\mathbf{s}}_n\hat{\mathbf{s}}_n^{\mathsf{H}}]\Bigg]^{-1}\Bigg). \tag{26}$$

As the CRLB is $\mathbf{J}^{-1}(\mathrm{Re}\,\mathbf{h}) = \frac{2\sigma_v^2}{N}tr\Bigg(\Bigg[E[\mathbf{s}_n\mathbf{s}_n^{\mathsf{H}}]\Bigg]^{-1}\Bigg)$, it follows that $E\left[\Delta\mathbf{h}^{\mathsf{H}}\Delta\mathbf{h}\right] > \mathbf{J}^{-1}(\mathrm{Re}\,\mathbf{h})$ i.e.,

$$E\left[\Delta\mathbf{h}^{\mathsf{H}}\Delta\mathbf{h}\right] > \frac{2\sigma_v^2}{N}tr\Bigg(\Bigg[E[\mathbf{s}_n\mathbf{s}_n^{\mathsf{H}}]\Bigg]^{-1}\Bigg). \tag{27}$$

which approaches the CRLB asymptotically for large N.

V. BLIND SYSTEM IDENTIFICATION OF MOVING AVERAGE MODEL USING EM-UKS ESTIMATOR

In the EM-UKS method, the complete data set ξ is given as:

$$\xi = \{s_0, \ldots, s_{N-1}, y_0, \ldots, y_{N-1}\} \tag{28}$$

The algorithm iterates between the following two steps until convergence is reached:

1) E-step: Compute

$$Q(\theta, \hat{\theta}_l) = E\{\xi|\theta_l\}$$

2) M-step: Solve

$$\hat{\theta}_{(l+1)} = \arg\max_\theta Q(\theta, \hat{\theta}_l). \tag{29}$$

Then we have,

$$\mathsf{P}(\mathbf{x}_0) = \mathcal{CN}(0, 2\sigma^2)$$
$$\mathsf{P}(y_n|\mathbf{s}_n) = \mathcal{CN}(\mathbf{h}^{\mathsf{H}}\mathbf{s}_n, 2\sigma_v^2) \tag{30}$$

Substituting the respective probability density functions from (30), the likelihood function of the complete data set ξ is given by:

$$\mathsf{P}(\xi|\theta) = \frac{1}{2\pi\sigma^2}\exp\left(\frac{-(\mathbf{x}_0\mathbf{x}_0^{\mathsf{H}})}{2\sigma^2}\right) \times\prod_{n=1}^{N}\frac{1}{2\pi\sigma_v^2}\exp\left(\frac{-(y_n - z_n)(y_n - z_n)^{\mathsf{H}}}{2\sigma_v^2}\right),$$
$$= \frac{1}{2\pi\sigma^2}\times\exp\left(\frac{-(\mathbf{x}_0\mathbf{x}_0^{\mathsf{H}})}{2\sigma^2}\right)\prod_{n=1}^{N}\frac{1}{2\pi\sigma_v^2} \times\exp\left(\frac{-(y_n - \mathbf{h}^{\mathsf{H}}\mathbf{s}_n)(y_n - \mathbf{h}^{\mathsf{H}}\mathbf{s}_n)^{\mathsf{H}}}{2\sigma_v^2}\right),$$
$$= \frac{1}{2\pi\sigma^2}\exp\left(\frac{-(\mathbf{x}_0\mathbf{x}_0^{\mathsf{H}})}{2\sigma^2}\right) \times\prod_{n=1}^{N}\frac{1}{2\pi\sigma_v^2}\exp\left(\frac{-(y_n - \mathbf{h}^{\mathsf{H}}\mathbf{s}_n)(y_n - \mathbf{h}^{\mathsf{H}}\mathbf{s}_n)^{\mathsf{H}}}{2\sigma_v^2}\right). \tag{31}$$

The log–likelihood function of the complete data set is expressed by:

$$\ell(\xi|\theta) = -\ln\,(2\pi\sigma^2) - N\ln(2\pi\sigma_v^2) - \frac{1}{2\sigma^2}\mathbf{x}_0\mathbf{x}_0^{\mathsf{H}} - \frac{1}{2\sigma_v^2}\left[[\sum_{n=1}^{N}(y_n - \mathbf{h}^{\mathsf{H}}\mathbf{s}_n)(y_n - \mathbf{h}^{\mathsf{H}}\mathbf{s}_n)^{\mathsf{H}}]\right]. \tag{32}$$

1) **E Step** : In the expectation step, the estimated parameters of the previous iteration is used and the expected value of the log likelihood function $\ell(\xi|\theta)$ ia calculated as:

$$Q_{(l)} = E[\ell(\xi|\theta)]. \tag{33}$$

The expectation Q is expressed as:

$$Q_l = -\ln(2\pi\sigma^2) - N\ln(2\pi\sigma_v^2) - \frac{1}{2\sigma^2}E[\mathbf{x}_0\mathbf{x}_0^{\mathsf{H}}|\mathbf{y};\theta] - \frac{1}{2\sigma_v^2}\left[\sum_{n=1}^{N}y_n y_n^{\mathsf{H}} - 2\sum_{n=1}^{N}y_n\mathbf{h}^{\mathsf{H}}E[\mathbf{s}_n|\mathbf{y};\theta]\right] - \frac{1}{2\sigma_v^2}\left[\sum_{n=1}^{N}\mathbf{h}^{\mathsf{H}}E[\mathbf{s}_n\mathbf{s}_n^{\mathsf{H}}|\mathbf{y};\theta]\mathbf{h}\right]. \tag{34}$$

Using the following expressions which are obtained from the UKS using the Rauch-Tung-Striebel smoothing procedure [45] we have,

$$\mathbf{s}_n^{smooth} = E[\mathbf{s}_n|\mathbf{y};\theta], \tag{35}$$
$$\mathbf{R}_n = E[\mathbf{s}_n\mathbf{s}_n^{\mathsf{H}}|\mathbf{y};\theta]. \tag{36}$$

Then the expectation turns into,

$$Q_{(l)} = -\ln(2\pi\sigma^2) - N\ln(2\pi\sigma_v^2) - \frac{1}{2\sigma^2}(\mathbf{x}_0^{smooth}\mathbf{x}_0^{smooth}) - \frac{1}{2\sigma_v^2}\left[\sum_{n=1}^{N} y_n y_n^{\mathsf{H}} - 2\mathbf{h}^{\mathsf{H}}\mathbf{s}_n^{smooth}\right] - \frac{1}{2\sigma_v^2}\left[\sum_{n=1}^{N}\mathbf{h}^{\mathsf{H}}\mathbf{R}_n\mathbf{h}\right]. \quad (37)$$

2. **M Step** = Using results from the previous steps, the estimation of the parameter set is performed given below as:

$$\hat{\theta}_{(l+1)} = \arg\max_{\theta} Q_l(\theta, \hat{\theta}_l). \quad (38)$$

The ML estimates are,

$$\widehat{\mathbf{h}} = \left[\mathbf{R_n}\right]^{-1}\sum_{n=1}^{N} y_n\hat{\mathbf{s}}_n^{smooth}, \quad (39)$$

$$\widehat{\sigma_v^2} = \frac{1}{N}\sum_{n=1}^{N} y_n(y_n - \widehat{\mathbf{h}}^{\mathsf{H}}\hat{\mathbf{s}}_n^{smooth}), \quad (40)$$

$$\widehat{x_0} = f_{\hat{\mathbf{s}}^{smooth}}^{-(N-1)}(\widehat{x}_{N-1}) \quad (41)$$

VI. PERFORMANCE EVALUATION

The performance metric in terms of MSE between the desired and the estimated channel coefficients is given by:

$$\text{MSE}_h = \frac{1}{K}\frac{\sum_{i=1}^{K}||\mathbf{h}_i - \hat{\mathbf{h}}_i||^2}{L} \quad (42)$$

where K is the number of iterations (trials) carried out for each signal to noise power ratio value defined as:

$$\text{SNR} = \frac{E[s_n^2]}{\sigma_v^2} \quad (43)$$

Unless otherwise stated, at each SNR $K = 30$ independent runs are carried out and in every run 10 EM iterations are used. The result is averaged over K runs. Another performance metric known as the Intersymbol Interference (ISI) is used to evaluate the equalization performance of a communication system. ISI measures how much of an impulse response's energy is in its strongest tap, defined by [46]:

$$\text{ISI} = \frac{||\mathbf{G}||^2 - \max_i|G_i|^2}{\max_i|G_i|^2} \quad (44)$$

In (44), $\mathbf{G}$ denotes the overall system impulse response coefficient vector after equalization expressed as: $\mathbf{G} = [g_1, \ldots, g_L]^{\mathsf{T}}$, where g_i is the i-th entry of $\mathbf{G}$, and $g_i = h * \hat{h}$ where $*$ denotes the convolution operator. Ideally, g_i should be equal to a delta function for perfect equalization to occur. As g_i gets closer to the delta function, the ISI becomes smaller. In other words, the smaller the ISI, the better an equalizer performs. We evaluate the equalization performance in terms of the mean squared error expressed as:

$$MSE_{eq} = \frac{1}{N}\sum_{n=1}^{N}(s_n - \hat{s}_n)^2 \quad (45)$$

Convergence is detected by computing the value of the log-likelihood after each iteration and halting when it appears not to be changing in a significant manner from one iteration to the next. The convergence threshold for EM iteration is set to 0.01.

A. RESULTS OF BLIND SYSTEM IDENTIFICATION USING RANDOM BINARY INPUT SIGNAL

In this section, we demonstrate the effectiveness of the proposed method in system identification of MA model of length $L = 3$ having parameters denoted by $h = [1, 0.6, 0.3]$. For the proposed method, the reverse interval mapping is performed on RS of length N that takes binary values $\{\pm 1\}$. The chaos representation of RS is performed on non-overlapping blocks of data of size $N^* = 16$. Such a block based approach during the reverse interval mapping prevents the mismatch between the chaotic symbolic signal (CS) obtained from the symbolic dynamics and the RS. Otherwise, the mismatch between the CS and RS leads to errors which may be amplified during the system identification procedure. The rationale for the block-based approach is further illustrated subsequently.

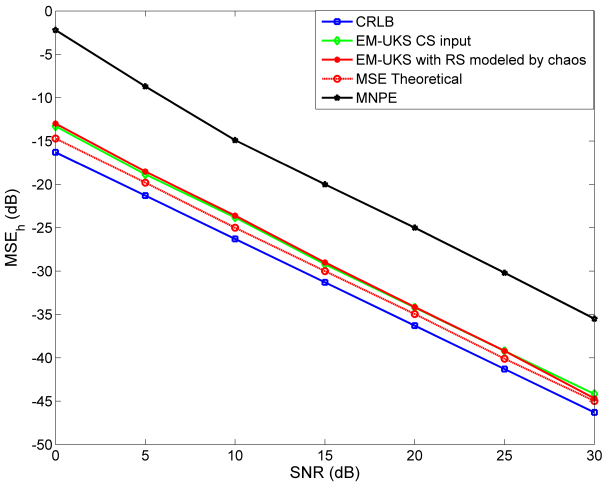

FIGURE 2. Comparison of MSE's for N = 128.

1) COMPARISON OF DERIVED MSE WITH CRLB

To evaluate the efficiency of our proposed approach (denoted as EM-UKS RS modeled by chaos in the graph), the theoretical MSE (MSE_h) is compared with the CRLB of chaos representation of RS in Fig. 2 which is obtained using $N = 128$ data points. We considered the MSE_h performance comparison with two kinds of input signal: a binary valued RS signal and the CS which is obtained by the PWL. Fig. 2 shows the MSE_h results using the methods EM-UKS with CS input [18], the Minimum Nonlinear Prediction Error (MNPE) [3] with CS and EM-UKS with the proposed approach (denoted as EM-UKS using RS modeled by chaos in the plot). From Fig. 2, it is observed that the MSE_h performance of EM-UKS using RS modeled by chaos method and EM-UKS using CS

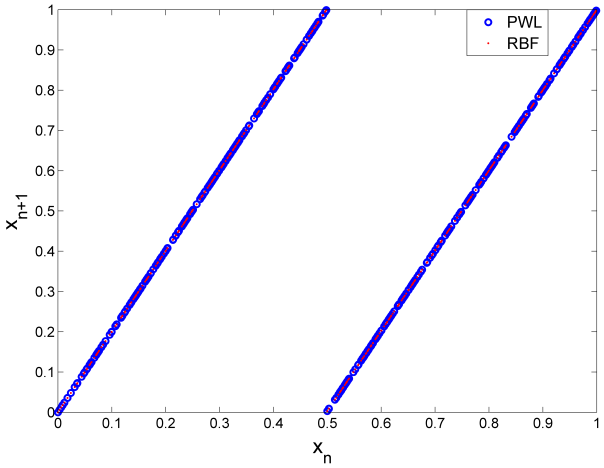

FIGURE 3. Approximated prediction function using an RBF network and the accurate prediction function.

as the input are almost similar. At SNR = 0 dB, there is a difference of about 1.8 dB between MSE_h of the proposed method and the theoretical MSE_h. At SNR = 15 dB, the MSE_h of EM-UKS using the proposed method lacks behind theoretical MSE_h by about 1 dB. Also, from Fig. 2 we can infer that at SNR = 0 dB the blind identification performance of our method is close to the CRLB with a difference of about 3.3 dB. Comparison of our method with MNPE shows significant performance improvement.

2) SYSTEM IDENTIFICATION PERFORMANCE WITH AN APPROXIMATED PREDICTION FUNCTION

We further considered the blind system identification performance of the proposed method without the knowledge of the chaotic map. The approximated PWL chaotic map shown in Fig. 3 is obtained by using a radial basis function (RBF) neural network. The RBF predictor is a three layer neural network with Gaussian hidden nodes. It is composed of an input layer, hidden nodes and the output layer. The output units implement a weighted sum of hidden unit outputs. The RBF network is trained using 128 examples to approximate the PWL chaotic map. The numbers of the neurons in the input, hidden, and output layers were 1, 2, and 1, respectively.

It can be observed from Fig. 4 that the EM-UKS with the proposed approach using an RBF provided an accurate identification of the MA model. The MSE_h performance using the approximate of the unknown PWL chaotic map is very close to that using the known PWL chaotic map. Therefore, the proposed approach can work with an unknown chaotic map as well.

3) EFFECT OF DATA LENGTH ON SYSTEM IDENTIFICATION PERFORMANCE

In Fig. 5, system identification performance of the proposed method is compared with EM-UKS using CS as the input, non-blind Least Squares (LS) and blind Constant Modulus

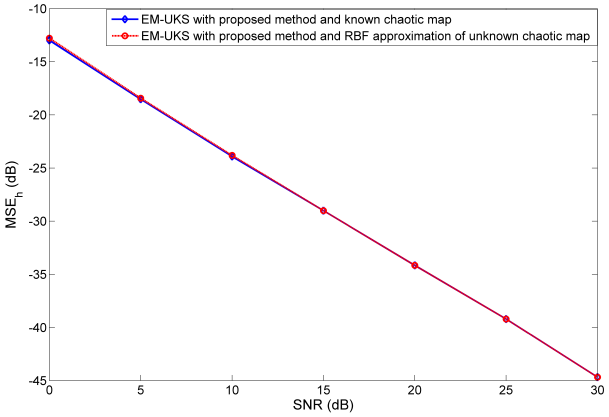

FIGURE 4. Comparison of system identification performance using PWL with RBF and known PWL.

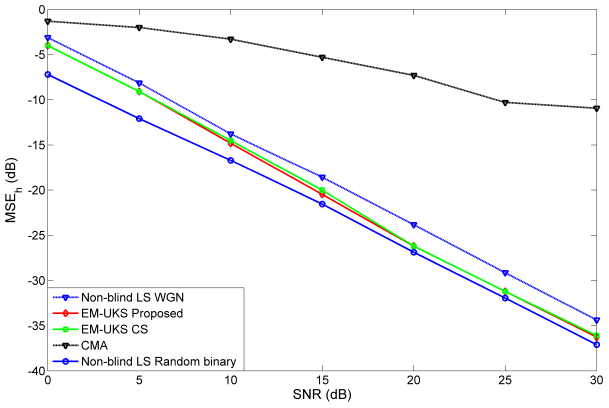

FIGURE 5. Comparison of MSE for N = 16.

Algorithm (CMA) methods. The MSE_h is calculated for a data length of $N = 16$. The step size for CMA was 0.001. The MSE performance of the proposed method is quite close to the MSE performance of non-blind LS using binary input with a difference of about 3.2 dB at SNR = 0 dB. In comparison to non-blind LS with numeric input (White Gaussian Noise (WGN)), the proposed method performs better at SNR = 0 dB with a difference of about 3 dB. In comparison with EM-UKS with CS input, the performance of the proposed method is quite similar to EM-UKS with CS. On the other hand, CMA performs poorly since it requires quite a large number of samples to give performance quite close to that of non-blind. From Fig. 5, it is observed that the proposed approach with EM-UKS shows superior system identification performance for a short data length of $N = 16$ in comparison to CMA. The results from Fig. 4 and Fig. 5 suggests that for the proposed method, using a block (window) of length N^* during chaos modeling of RS yields estimation performance quite close to the EM-UKS with CS and non-blind LS techniques. The proposed approach can be applied to general signals and does not require larger data volumes for the same signal estimation quality as that of non-blind.

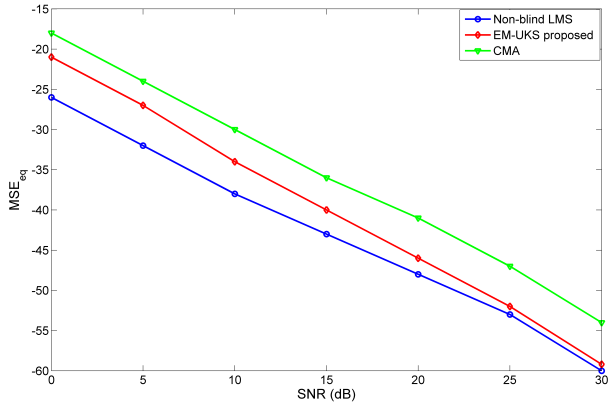

FIGURE 6. Comparison of binary signal recovery MSE's for $N = 10^4$.

4) COMPARISON OF BLIND EQUALIZATION FOR BINARY DATA WITH NON-BLIND LEAST MEAN SQUARES AND BLIND CONSTANT MODULUS ALGORITHM

Fig. 6 shows the performance comparison of estimation of the input signal. The MSE_{eq} of the proposed method using EM-UKS is plotted in Fig. 6 by using sliding blocks of $N^* = 16$ data points over $N = 10^4$ and $K = 300$. The parameter settings (step size, μ) for CMA = 0.001 and non-blind Least Mean Squares (LMS) = 0.015. Comparison of the proposed method using EM-UKS with the non-blind LMS method shows that the proposed method lacks behind non-blind LMS by 5 dB at SNR = 0 dB, with performance increasing gradually and approaching close to the non-blind LMS at high SNR. At SNR = 15 dB, the MSE of the proposed method lacks behind non-blind LMS by about 3 dB. However, at SNR = 30 dB, the MSE of the proposed method differs by about 1 dB from the non-blind LMS. On the other hand CMA shows poor equalization performance compared to the proposed method. At SNR = 0 dB, CMA lacks behind non-blind LMS by about 11 dB. Due to the knowledge of the transmitted sequence, the non-blind LMS algorithm has a better performance.

Fig. 7(a) shows the plot of first 50 data points of the RS for $N = 256$ data points by using sliding blocks of length $N^* = 16$ at SNR = 30 dB. Fig. 7(b) is the recovered RS using EM-UKS with the proposed method.

B. PERFORMANCE EVALUATION IN BLIND CHANNEL EQUALIZATION IN COMMUNICATIONS

In this section, we extend our proposed approach from binary RS to muti-level RS in an application to blind channel equalization for a QAM communication system. Based on the input RS, a PWL chaotic map is created to model the RS. Here the information signal takes symbols that represents the amplitude levels for M-QAM modulation technique. The RS is modeled by the PWL that is adjusted for $m = \sqrt{M}$ symbols. The RS contains $a_1, a_2, \ldots, a_m$ unique symbols with equal probability of occurrence of symbols $p_1, p_2, \ldots, p_m$. The chaos representation is performed to the real and imaginary

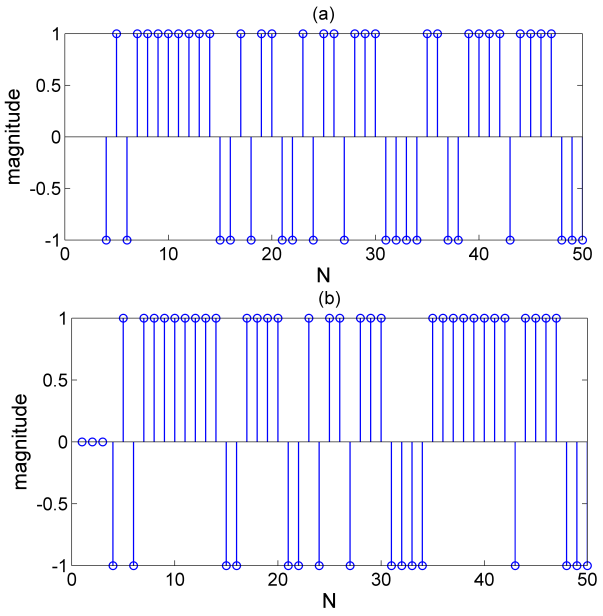

FIGURE 7. Simulation result at SNR = 30 dB (a) Input RS, (b) Estimated input using EM-UKS with the proposed method.

component and an identical PWL map is generated for the real and imaginary component of the RS. For the application to blind channel equalization for 64 QAM communication, the PWL is partitioned into $m = 8$ disjoint regions $I = \{I_1, I_2, \ldots, I_m\}$, $\cup_{k=1}^{m} I_k = I$ with symbols and is defined by:

$$f(x) = \begin{cases} \dfrac{x}{p_1}, x \in I_1 \\ \dfrac{x - p_1}{p_2}, x \in I_2 \\ \ldots \\ \dfrac{x - \sum_{k=1}^{m-1} p_k}{p_m}, x \in I_m \end{cases} \tag{46}$$

where the intervals I_k $(k = 1, 2, \ldots, m)$ map to the distinct symbols a_k $(k = 1, 2, \ldots, m)$. These intervals are determined by:

$$\begin{aligned} I_1 &= [0, p_1], p_0 = 0, \\ I_k &= [\sum_{j=0}^{k-1} p_j, \sum_{j=0}^{k} p_j], k = 1, 2, 3, \ldots, m \end{aligned} \tag{47}$$

that is adjusted to the symbol probabilities of a RS. The PWL for this application is shown in Fig. 8 where each interval represents a unique symbol. Therefore, we have two PWL constructed for modelling the real and imaginary components of the QAM signal. The chaotic representation starts by using the inverse interval mapping as follows:

$$f_{s_n}^{-1}(x_{n+1}) = \begin{cases} p_1 \times x_{n+1}, \text{for } s_n = a_1, \\ \ldots \\ \sum_{k=1}^{(m-1)}(p_k) + p_m \times x_{n+1}, s_n = a_m. \end{cases} \tag{48}$$

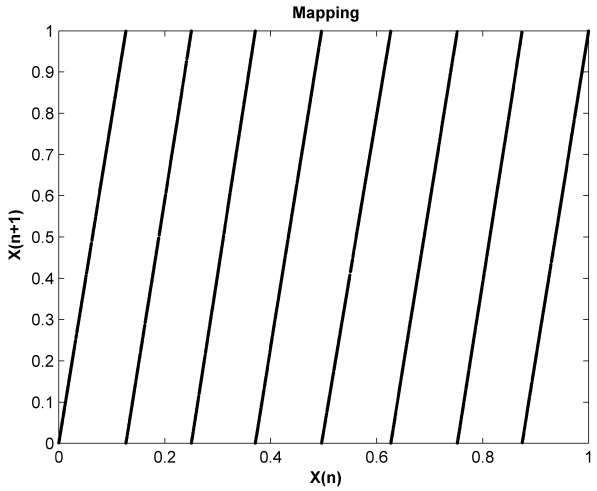

FIGURE 8. Plot of PWL for $m = 8$ symbols.

$$\begin{aligned} s_n = \Theta(x_n) &= a_1, \text{ if } x_n \in I_1 \\ &= a_2, \text{ if } x_n \in I_2 \\ &\vdots \\ &\vdots \\ &= a_m, \text{ if } x_n \in I_m. \end{aligned} \tag{49}$$

The channel is modeled as an FIR system representing a multipath Rayleigh fading channel with L paths. The coefficients take values from the complex domain. Each of the imaginary and real component's of the coefficients is a Gaussian random variable with variance of 0.5 each. The complex channel coefficients are randomly generated. The equalizer is also an FIR system with L coefficients. Here, the performance assessment of blind channel equalization using the proposed approach is discussed. We show comparison of the proposed chaos-based equalizers using EM-UKS and EM-EKS estimation methods with equalizers for QAM communication – Multi Modulus Algorithm (MMA) [47] and Multi Constant Modulus Algorithm (MCMA) [48]. We also compare with the non-blind LS estimator. Fig. 9 depicts the block diagram of the proposed method.

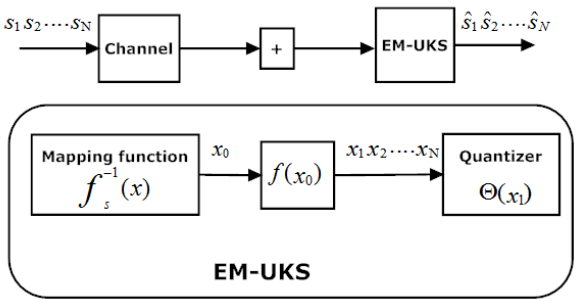

FIGURE 9. Proposed methodology for channel equalization using chaos.

1) EFFECT OF NOISE IN CHANNEL EQUALIZATION

For each SNR, the MSE_h is calculated by averaging over $K = 100$ with 50 EM iterations using $N = 256$ data points.

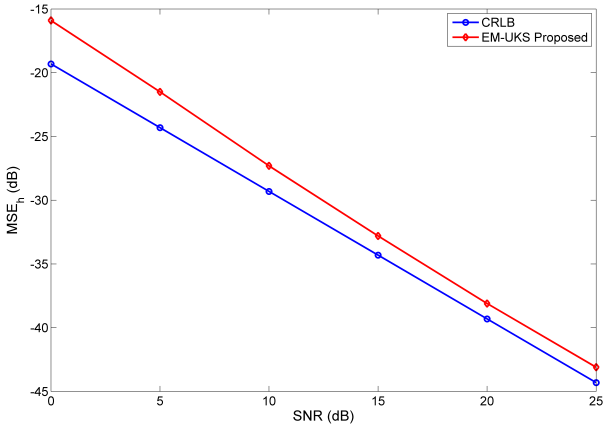

FIGURE 10. Comparison of MSE of the proposed method with the CRLB for $N = 256$.

Performance of the proposed method in noise is shown in Fig. 10 for $L = 3$ and is compared to the CRLB. It is observed that at low SNR, there is a difference of about 3.4 dB between the CRLB and the MSE_h after which the MSE_h performance of the proposed approach gradually approaches towards the CRLB at high SNR.

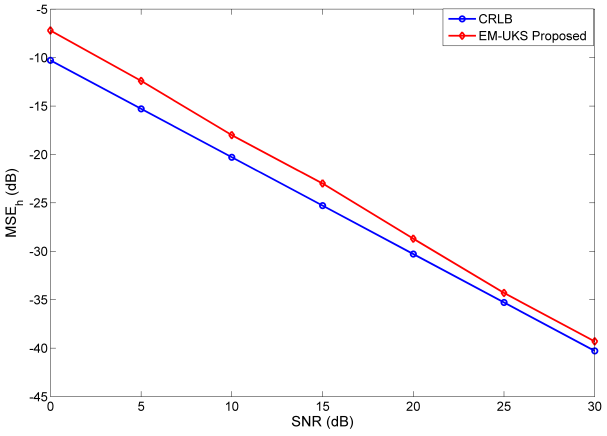

FIGURE 11. Comparison of MSE for $N = 32$.

2) EFFECT OF DATA LENGTH

A sliding window each of length N^* is applied. By experiments, we found that $N^* = 32$ gives good estimation performance. The comparison of channel estimation performance, MSE_h using EM-UKS with CRLB for $N = 32$ is shown in Fig. 11 using 10 EM iterations. At SNR $= 0$ dB, MSE_h of the proposed method is behind CRLB by about 3 dB. At SNR$>$ 10 dB, this difference reduces to approximately 2 dB and at SNR $= 30$ dB, there is a difference of about 1 dB between the MSE_h and CRLB. Fig. 12 shows the plot of negative of the log likelihood vs. number of EM iterations for a sequence of length $N = 32$. The proposed method demonstrates fast convergence behavior for short sequence length. Therefore, we use data of short sequence, called

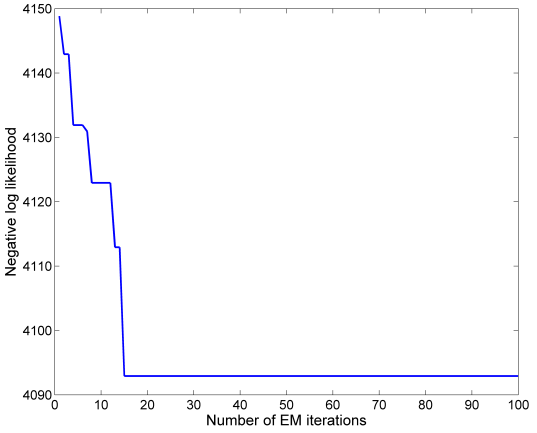

FIGURE 12. Convergence behavior of the algorithm.

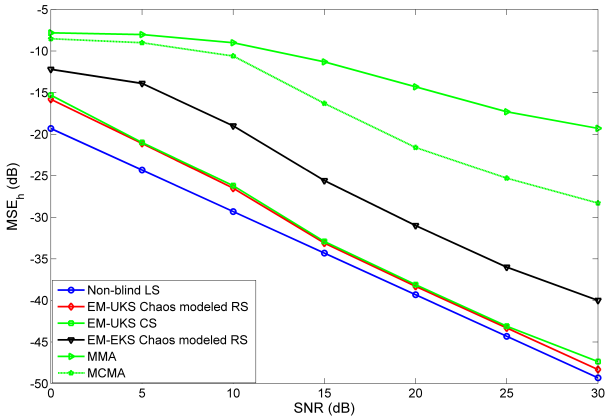

FIGURE 13. Comparison of channel estimation using non-blind LS, MCMA, MMA, EM-UKS with CS EM-EKS and EM-UKS with chaos for $N = 256$.

as the block (window) of length $N^* = 32$ data points during reverse interval mapping and then concatenate them after all the blocks have been modeled by chaos for both EM-EKS [36] and EM-UKS.

3) COMPARISON WITH BLIND EM-UKS, EM-EKS, MMA, MCMA, AND NON-BLIND LS

For comparison with EM-EKS, the QAM symbols at the receiver is also represented by inverse interval mapping processing N^* data points. Given the transmitted signal's constellation size $m = 8$, and $L = 5$ for each SNR, we run $K = 300$ simulations. The step size of the MMA and MCMA methods are set as 0.01 and 0.5 respectively (the best value in our experience). The equalizer length for MMA and MCMA are set as $2L - 1$. 50 EM iterations are used. Fig. 13 demonstrates the performance comparison of EM-UKS with EM-EKS, MMA and MCMA and non-blind LS for $N = 256$. The graph for non-blind LS in Fig. 13 is plotted assuming that the channel parameters are known. We have observed that since MMA and MCMA are adaptive algorithms, they require more data points for convergence and to accurately yield channel coefficients whereas our proposed method can work for short data sequences yielding better accuracy as well. At low SNR of 0 dB, the proposed method with EM-UKS lacks behind the non-bind LS by about 3.5 dB. In comparison with MMA and MCMA, at SNR = 0 dB our method with EM-UKS shows an improvement of about 8 dB and 7 dB respectively. The proposed method with EM-UKS shows a superior estimation performance increase at high SNR all throughout. On the other hand, the proposed method using EM-EKS estimator at SNR = 0 dB lacks behind MMA and MCMA by approximately 3 dB and 4 dB respectively. Clearly, our proposed method with EM-UKS equalizer closely follows the non-blind LS at all levels of SNR. Fig. 14 shows the ISI values obtained for several values of SNR for channel length $L = 5$. From Fig. 14, we can observe that for low and high SNR values, the performance of the proposed method with EM-UKS is close to the non-blind. For moderate values of SNR, EM-EKS and EM-UKS perform similarly. However, MNPE yields poor results in comparison to the proposed approach. The experiment was repeated for channel length $L = 10$ and the result is given in Fig. 15. In Fig. 16,

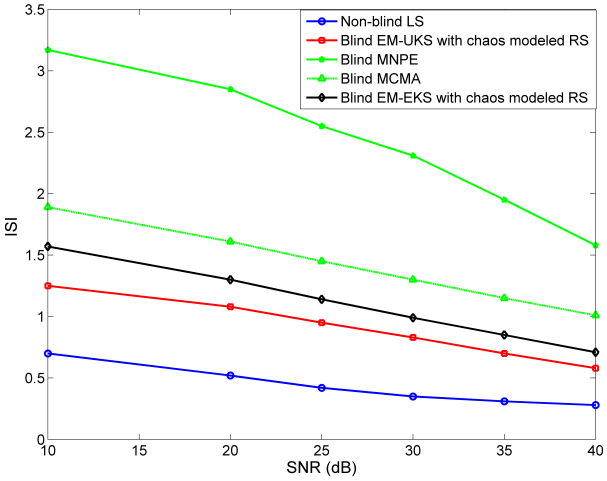

FIGURE 14. Comparison of Equalization performance in terms of ISI for $L = 5$.

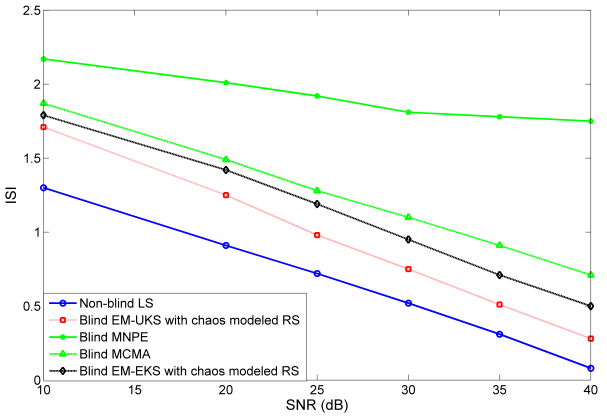

FIGURE 15. Comparison of equalization performance in terms of ISI for $L = 10$.

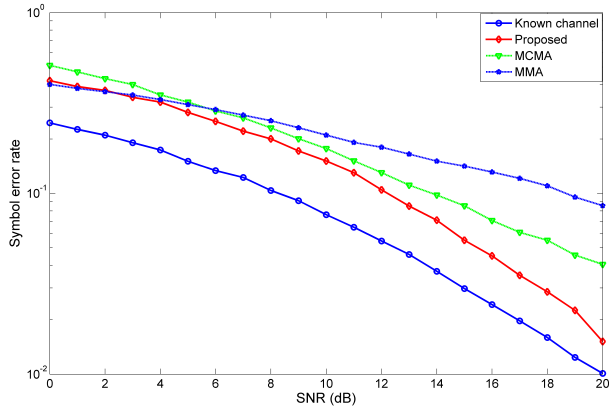

FIGURE 16. Signal recovery performance comparison for $N = 10^4$.

the performance of recovering the transmitted signal is compared with traditional blind equalizers. The graph is obtained using $N = 10^4$ and $K = 100$. The recovered signal is the equalized source input. It can be clearly seen from Fig. 16 that at low SNR, the performance of the proposed method is quite close to the MMA and MCMA. The performance of EM-UKS gradually tends towards the non-blind LS performance at high SNR and outperforms the MMA and MCMA methods.

VII. CONCLUSION

In this paper, we propose to apply chaos to represent random symbolic data for signal processing applied to a blind system identification problem. The derived analytical results lay the foundation that the blind estimation performance of a random information signal modeled by chaos is optimal in comparison to non-blind estimation method for random information signal. Simulation results support our idea that system identification using chaos can be applied to enhance blind equalization at low and high SNR for general random binary symbols.

However, a limitation of our approach is an increase in the computation time due to the backward recursion in the chaos representation of RS. But considering the improvement shown in system identification by the proposed approach, this limitation can be overcome by faster processors and memory. Our approach opens a promising new direction of an alternate way of using the merits of chaos in signal processing. This claim is supported by analytical and simulation results which are summarized as follows:

- The blind estimation performance of the chaos representation of RS is comparable to the optimal identification performance imposed by the CRLB of the non-blind.
- The lower bound on the derived MSE for our proposed approach is found to achieve the derived CRLB.
- The proposed method is also applicable for a small data sequence.
- The proposed method can be extended by increasing or decreasing the number of partitions of the chaotic map.

APPENDIX
DERIVATION OF THE CRLB

The presence of Re(·) and Im(·) in the parameter vector indicates that θ and θ^* are to be treated as being functionally independent parameters. We recall from (16) that the complex CRLB is connected to the real CRLB by the relation $\mathrm{CRLB}(\theta^*) = [\mathbf{T}^{\mathsf{H}}]^{-1}\mathrm{CRLB}(\mathrm{Re}\,\theta)\mathbf{T}^{-1}$ We first derive the CRLB for the complex case followed by the CRLB for the real case for blind estimation using chaos representation of random symbolic sequence.

A. CRLB FOR DATA IN COMPLEX DOMAIN

To derive the CRLB, the FIM is of size 5 by 5 given as:

$$\mathbf{J}(\mathrm{Re}\,\theta) = -E\begin{bmatrix} J_{11} & J_{12} & J_{13} & J_{14} & J_{15} \\ J_{21} & J_{22} & J_{23} & J_{24} & J_{25} \\ J_{31} & J_{32} & J_{33} & J_{34} & J_{35} \\ J_{41} & J_{42} & J_{43} & J_{44} & J_{45} \\ 0 & 0 & 0 & 0 & J_{55} \end{bmatrix} \tag{50}$$

The first and second order partial derivatives are:

$$\text{(a)}\ \frac{\partial \ell(\mathbf{y}|\theta)}{\partial\,\mathrm{Re}\,\mathbf{h}} = \frac{1}{\sigma_v^2}[\sum_{n=1}^{N} y_n \mathbf{s}_n^{\mathsf{H}} - \mathrm{Re}\,\mathbf{h}^{\mathsf{H}} \sum_{n=1}^{N} \mathbf{s}_n \mathbf{s}_n^{\mathsf{H}}]$$

$$\text{(b)}\ \frac{\partial \ell(\mathbf{y}|\theta)}{\partial\,\mathrm{Im}\,\mathbf{h}} = \frac{1}{\sigma_v^2}[\sum_{n=1}^{N} y_n \mathbf{s}_n^{\mathsf{H}} - \mathrm{Im}\,\mathbf{h}^{\mathsf{H}} \sum_{n=1}^{N} \mathbf{s}_n \mathbf{s}_n^{\mathsf{H}}]$$

$$\text{(c)}\ \frac{\partial \ell(\mathbf{y}|\theta)}{\partial\,\mathrm{Re}\,x_0} = \frac{1}{\sigma_v^2}[\sum_{n=0}^{N-1} (y_n - \mathbf{h}^{\mathsf{H}}\mathbf{s}_n)\mathbf{h}^{\mathsf{H}}\,\mathrm{Re}\,\mathbf{x}_n'^{\mathsf{H}}]$$

$$\text{(d)}\ \frac{\partial \ell(\mathbf{y}|\theta)}{\partial\,\mathrm{Im}\,x_0} = \frac{1}{\sigma_v^2}[\sum_{n=0}^{N-1} (y_n - \mathbf{h}^{\mathsf{H}}\mathbf{s}_n)\mathbf{h}^{\mathsf{H}}\,\mathrm{Im}\,\mathbf{x}_n'^{\mathsf{H}}]$$

$$\text{(e)}\ \frac{\partial \ell(\mathbf{y}|\theta)}{\partial \sigma_v} = -\frac{2N}{\sigma_v} + \frac{1}{\sigma_v^3}\sum_{n=0}^{N-1} \left((y_n - \mathbf{h}^{H}\mathbf{s}_n)^{\mathsf{H}}(y_n - \mathbf{h}^{\mathsf{H}}\mathbf{s}_n)\right)$$

For ease of representation, the block matrices are represented as follows:

$$\text{(f)}\ \mathbf{J}_{11} = \frac{\partial^2 \ell(\mathbf{y},\theta)}{\partial^2\,\mathrm{Re}\,\mathbf{h}} = -\frac{1}{\sigma_v^2}\sum_{n=0}^{N-1} \mathbf{s}_n \mathbf{s}_n^{\mathsf{H}}$$

$$\text{(g)}\ \mathbf{J}_{12} = \frac{\partial^2 \ell(\mathbf{y},\theta)}{\partial\,\mathrm{Re}\,\mathbf{h}\partial\,\mathrm{Im}\,\mathbf{h}} = 0$$

as there is no imaginary component of $\mathbf{h}$ in the term $\mathrm{Re}\,\mathbf{h}$

$$\text{(h)}\ \mathbf{J}_{13} = \frac{\partial^2 \ell(\mathbf{y},\theta)}{\partial\,\mathrm{Re}\,\mathbf{h}\partial\,\mathrm{Re}\,x_0} = \frac{1}{\sigma_v^2}\sum_{n=0}^{N-1}(y_n\mathbf{s}_n - 2\,\mathrm{Re}\,\mathbf{h}^{\mathsf{H}}\mathbf{s}_n\,\mathrm{Re}\,\mathbf{x}_n'^{\mathsf{H}})$$

$$\text{(i)}\ \mathbf{J}_{14} = \frac{\partial^2 \ell(\mathbf{y},\theta)}{\partial\,\mathrm{Re}\,\mathbf{h}\partial\,\mathrm{Im}\,x_0} = \frac{1}{\sigma_v^2}\sum_{n=0}^{N-1}(y_n\mathbf{s}_n - 2\,\mathrm{Re}\,\mathbf{h}^{\mathsf{H}}\mathbf{s}_n\,\mathrm{Im}\,\mathbf{x}_n'^{\mathsf{H}})$$

$$\text{(j)}\ \mathbf{J}_{15} = \frac{\partial^2 \ell(\mathbf{y},\theta)}{\partial\,\mathrm{Re}\,\mathbf{h}\partial\sigma_v} = 0$$

(Since v_n is a zero mean Gaussian sequence, when we take the expectation all the terms that contain v_n will become zero)

$$\text{(k) } \mathbf{J}_{21} = \frac{\partial^2 \ell(\mathbf{y}|\theta)}{\partial \operatorname{Im}\mathbf{h} \partial \operatorname{Re}\mathbf{h}} = 0$$

as there is no real component of $\mathbf{h}$ in the term $\operatorname{Im}\mathbf{h}$

$$\text{(l) } \mathbf{J}_{22} = \frac{\partial^2 \ell(\mathbf{y}|\theta)}{\partial^2 \operatorname{Im}\mathbf{h}} = -\frac{1}{\sigma_v^2}\sum_{n=0}^{N-1} \mathbf{s}_n \mathbf{s}_n^{\mathsf{H}}$$

$$\text{(m) } \mathbf{J}_{23} = \frac{\partial^2 \ell(\mathbf{y}|\theta)}{\partial \operatorname{Im}\mathbf{h} \partial \operatorname{Re} x_0} = j\frac{1}{\sigma_v^2} \operatorname{Im}\mathbf{h}^{\mathsf{H}} \sum_{n=0}^{N-1} 2\mathbf{s}_n \operatorname{Re}\mathbf{x}'^{\mathsf{H}}_n$$

$$\text{(n) } \mathbf{J}_{24} = \frac{\partial^2 \ell(\mathbf{y}|\theta)}{\partial \operatorname{Im}\mathbf{h} \partial \operatorname{Im} x_0} = j\frac{1}{\sigma_v^2} \operatorname{Im}\mathbf{h}^{\mathsf{H}} \sum_{n=0}^{N-1} 2(\mathbf{s}_n \operatorname{Im}\mathbf{x}'^{\mathsf{H}}_n)$$

$$\text{(o) } \mathbf{J}_{25} = \frac{\partial^2 \ell(\mathbf{y}|, \theta)}{\partial \operatorname{Im}\mathbf{h} \partial \sigma_v} = 0$$

(Since v_n is a zero mean Gaussian sequence, when we take the expectation all the terms that contain v_n will become zero)

$$\begin{aligned}\text{(p) } \mathbf{J}_{31} &= \frac{\partial^2 \ell(\mathbf{y}|\theta)}{\partial \operatorname{Re} x_0 \partial \operatorname{Re}\mathbf{h}} \\ &= \frac{1}{\sigma_v^2}\sum_{n=0}^{N-1} (y_n \operatorname{Re}\mathbf{x}'_n - \operatorname{Re}\mathbf{s}_n[\operatorname{Re}\mathbf{s}_n]^{\mathsf{H}} \operatorname{Re}\mathbf{h})\end{aligned}$$

$$\begin{aligned}\text{(q) } \mathbf{J}_{32} &= \frac{\partial^2 \ell(\mathbf{y}|\theta)}{\partial \operatorname{Re} x_0 \partial \operatorname{Im}\mathbf{h}} \\ &= \frac{1}{\sigma_v^2}\sum_{n=0}^{N-1} (y_n \operatorname{Re}\mathbf{x}'_n - \operatorname{Re}\mathbf{s}_n[\operatorname{Re}\mathbf{s}_n]^{\mathsf{H}} \operatorname{Im}\mathbf{h})\end{aligned}$$

$$\begin{aligned}\text{(r) } \mathbf{J}_{33} &= \frac{\partial^2 \ell(\mathbf{y}|\theta)}{\partial^2 \operatorname{Re} x_0} \\ &= \frac{1}{\sigma_v^2}\sum_{n=0}^{N-1} \left(v_n \mathbf{h}^{\mathsf{H}} \operatorname{Re}\mathbf{x}''_n - (\mathbf{h}^{\mathsf{H}} \operatorname{Re}\mathbf{x}'_n)(\mathbf{h}^{H} \operatorname{Re}\mathbf{x}'_n)^{\mathsf{H}}\right)\end{aligned}$$

$$\text{(s) } \mathbf{J}_{34} = \frac{\partial^2 \ell(\mathbf{y}|\theta)}{\partial \operatorname{Re} x_0 \partial \operatorname{Im} x_0} = \sum_{n=0}^{N-1} \mathbf{h}^{\mathsf{H}} \operatorname{Im}\mathbf{x}'_n \operatorname{Re}\mathbf{x}'_n \mathbf{h}^{\mathsf{H}} = 0$$

due to mathematical expectation operator

$$\text{(t) } \mathbf{J}_{35} = \frac{\partial^2 \ell(\mathbf{y}|\theta)}{\partial \operatorname{Re} x_0 \partial \sigma_v} = 0$$

(Since v_n is a zero mean Gaussian sequence, when we take the expectation all the terms that contain v_n will become zero)

$$\begin{aligned}\text{(u) } \mathbf{J}_{41} &= \frac{\partial^2 \ell(\mathbf{y}|\theta)}{\partial \operatorname{Im} x_0 \partial \operatorname{Re}\mathbf{h}} \\ &= \frac{1}{\sigma_v^2}\sum_{n=0}^{N-1} (y_n \operatorname{Im}\mathbf{x}'_n - \operatorname{Im}\mathbf{s}_n[\operatorname{Im}\mathbf{s}_n]^{\mathsf{H}} \operatorname{Re}\mathbf{h})\end{aligned}$$

$$\begin{aligned}\text{(v) } \mathbf{J}_{42} &= \frac{\partial^2 \ell(\mathbf{y}|\theta)}{\partial \operatorname{Im} x_0 \partial \operatorname{Im}\mathbf{h}} \\ &= \frac{1}{\sigma_v^2}\sum_{n=0}^{N-1} (y_n \operatorname{Im}\mathbf{x}'_n - \operatorname{Im}\mathbf{s}_n[\operatorname{Im}\mathbf{s}_n]^{\mathsf{H}} \operatorname{Im}\mathbf{h})\end{aligned}$$

where $x'_n = (f_{s_n}^{-1})(x_n)'$ and $\sum_{n=0}^{N-1} v_n^2 = 2N\sigma_v^2$.

$$\text{(w) } \mathbf{J}_{43} = \frac{\partial^2 \ell(\mathbf{y}|\theta)}{\partial \operatorname{Im} x_0 \partial \operatorname{Re} x_0} = \sum_{n=0}^{N-1} \mathbf{h}^{\mathsf{H}} \operatorname{Re}\mathbf{x}'_n \operatorname{Im}\mathbf{x}'_n \mathbf{h}^{\mathsf{H}} = 0$$

due to mathematical expectation operator

$$\begin{aligned}\text{(x) } \mathbf{J}_{44} &= \frac{\partial^2 \ell(\mathbf{y}|\theta)}{\partial^2 \operatorname{Im} x_0} \\ &= \frac{1}{\sigma_v^2}\sum_{n=0}^{N-1} \left(v_n \mathbf{h}^{\mathsf{H}} \operatorname{Im}\mathbf{x}''_n - (\mathbf{h}^{\mathsf{H}} \operatorname{Im}\mathbf{x}'_n)(\mathbf{h}^{\mathsf{H}} \operatorname{Im}\mathbf{x}'_n)^{\mathsf{H}}\right)\end{aligned}$$

$$\text{(y) } \mathbf{J}_{45} = \frac{\partial^2 \ell(\mathbf{y}|\theta)}{\partial \operatorname{Im} x_0 \partial \sigma_v} = 0.$$

$$\text{(z) } \mathbf{J}_{55} = \frac{\partial^2 \ell(\mathbf{y}|\theta)}{\partial^2 \sigma_v} = \frac{2N}{\sigma_v^2} - \frac{3}{\sigma_v^4}\sum_{n=0}^{N-1} \left(v_n v_n^{\mathsf{H}}\right) = -\frac{4N}{\sigma_v^2}$$

Note : $E[\sum_{n=0}^{N-1} v_n \mathbf{h}^{\mathsf{H}} \operatorname{Re}\mathbf{x}''_n] = 0, E[\sum_{n=0}^{N-1} v_n \mathbf{h}^{\mathsf{H}} \operatorname{Im}\mathbf{x}''_n] = 0$, $E[\sum_{n=0}^{N-1} y_n \operatorname{Re}\mathbf{x}'_n] = 0$, $\frac{\partial^2 \ell(\mathbf{y}|\theta)}{\partial \operatorname{Re}\mathbf{h} \partial \operatorname{Im}\mathbf{h}} = 0$, $\frac{\partial^2 \ell(\mathbf{y},\theta)}{\partial \operatorname{Im}\mathbf{h} \partial \operatorname{Re}\mathbf{h}} = 0$. We evaluate the following terms present in (16):

$$\mathbf{T}^{-1} = \begin{bmatrix} 1 & 1 & 0 & 0 & 0 \\ -1j & 1j & 0 & 0 & 0 \\ 0 & 0 & 1 & 1 & 0 \\ 0 & 0 & -1j & 1j & 0 \\ 0 & 0 & 0 & 0 & 1 \end{bmatrix} \tag{51}$$

and the other term $\left[\mathbf{T}^{\mathsf{H}}\right]^{-1}$ is evaluated as

$$[\mathbf{T}^{\mathsf{H}}]^{-1} = \begin{bmatrix} 1 & 1j & 0 & 0 & 0 \\ 1 & -1j & 0 & 0 & 0 \\ 0 & 0 & 1 & 1j & 0 \\ 0 & 0 & 1 & -1j & 0 \\ 0 & 0 & 0 & 0 & 1 \end{bmatrix} \tag{52}$$

For ease of representation, let

$$\mathbf{J}_{11} = \frac{1}{\sigma_v^2} E \sum_{n=0}^{N-1} \mathbf{s}_n \mathbf{s}_n^{\mathsf{H}}, \tag{53}$$

$$\mathbf{J}_{13} = \frac{2}{\sigma_v^2} E \sum_{n=0}^{N-1} (\operatorname{Re}\mathbf{h}^{\mathsf{H}} \mathbf{s}_n \operatorname{Re}\mathbf{x}'^{\mathsf{H}}_n), \tag{54}$$

$$\mathbf{J}_{14} = \frac{2}{\sigma_v^2} E \sum_{n=0}^{N-1} (\operatorname{Re}\mathbf{h}^{\mathsf{H}} \mathbf{s}_n \operatorname{Im}\mathbf{x}'^{\mathsf{H}}_n), \tag{55}$$

$$\mathbf{J}_{22} = \frac{1}{\sigma_v^2} E \sum_{n=0}^{N-1} \mathbf{s}_n \mathbf{s}_n^{\mathsf{H}}, \tag{56}$$

$$\mathbf{J}_{23} = j\frac{2}{\sigma_v^2} \operatorname{Im}\mathbf{h}^{\mathsf{H}} E(\sum_{n=0}^{N-1} \mathbf{s}_n \operatorname{Re}\mathbf{x}'^{\mathsf{H}}_n), \tag{57}$$

$$\mathbf{J}_{24} = j\frac{2}{\sigma_v^2} \operatorname{Im}\mathbf{h}^{\mathsf{H}} E \sum_{n=0}^{N-1} (\mathbf{s}_n \operatorname{Im}\mathbf{x}'^{\mathsf{H}}_n), \tag{58}$$

$$\mathbf{J}_{31} = \frac{1}{\sigma_v^2} E \sum_{n=0}^{N-1} (\mathrm{Re}\,\mathbf{s}_n [\mathrm{Re}\,\mathbf{s}_n]^{\mathsf{H}} \mathrm{Re}\,\mathbf{h}), \tag{59}$$

$$\mathbf{J}_{32} = \frac{1}{\sigma_v^2} E \sum_{n=0}^{N-1} (\mathrm{Re}\,\mathbf{s}_n [\mathrm{Re}\,\mathbf{s}_n]^{\mathsf{H}} \mathrm{Im}\,\mathbf{h}), \tag{60}$$

$$\mathbf{J}_{33} = \frac{1}{\sigma_v^2} E \sum_{n=0}^{N-1} (\mathbf{h}^{\mathsf{H}} \mathrm{Re}\,\mathbf{x}'_n)(\mathbf{h}^{\mathsf{H}} \mathrm{Re}\,\mathbf{x}'_n)^{\mathsf{H}}, \tag{61}$$

$$\mathbf{J}_{41} = \frac{1}{\sigma_v^2} E \sum_{n=0}^{N-1} (\mathrm{Im}\,\mathbf{s}_n [\mathrm{Im}\,\mathbf{s}_n]^{\mathsf{H}} \mathrm{Re}\,\mathbf{h}), \tag{62}$$

$$\mathbf{J}_{42} = \frac{1}{\sigma_v^2} E \sum_{n=0}^{N-1} (\mathrm{Im}\,\mathbf{s}_n [\mathrm{Im}\,\mathbf{s}_n]^{\mathsf{H}} \mathrm{Im}\,\mathbf{h}), \tag{63}$$

$$\mathbf{J}_{44} = \frac{1}{\sigma_v^2} E \sum_{n=0}^{N-1} (\mathbf{h}^{\mathsf{H}} \mathrm{Im}\,\mathbf{x}'_n)(\mathbf{h}^{\mathsf{H}} \mathrm{Im}\,\mathbf{x}'_n)^{\mathsf{H}} \tag{64}$$

Then, $[\mathbf{T}^{\mathsf{H}}]^{-1}[\mathbf{J}(\mathrm{Re}\,\theta)]^{-1}\mathbf{T}^{-1}$ yields the CRLB for the complex case expressed as,

$$var(\theta^* - \hat{\theta}^*) \geq \begin{bmatrix} 2 & 0 & 0 & 0 & 0 \\ 0 & 2 & 0 & 0 & 0 \\ 0 & 0 & 2 & 0 & 0 \\ 0 & 0 & 0 & 2 & 0 \\ 0 & 0 & 0 & 0 & 1 \end{bmatrix} [\mathbf{J}(\mathrm{Re}\,\theta)]^{-1} \tag{65}$$

where

$$[\mathbf{J}(\mathrm{Re}\,\theta)]^{-1} = \begin{pmatrix} \mathbf{J}_{11} & 0 & \mathbf{J}_{13} & \mathbf{J}_{14} & 0 \\ 0 & \mathbf{J}_{22} & \mathbf{J}_{23} & \mathbf{J}_{24} & 0 \\ \mathbf{J}_{31} & \mathbf{J}_{32} & \mathbf{J}_{33} & 0 & 0 \\ \mathbf{J}_{41} & \mathbf{J}_{42} & 0 & \mathbf{J}_{44} & 0 \\ 0 & 0 & 0 & 0 & \frac{4N}{\sigma_v^2} \end{pmatrix}^{-1} \tag{66}$$

$$= \begin{bmatrix} \begin{bmatrix} \mathbf{J}_{11} & 0 \\ 0 & \mathbf{J}_{22} \end{bmatrix}^{-1} \begin{bmatrix} \mathbf{J}_{13} & \mathbf{J}_{14} \\ \mathbf{J}_{23} & \mathbf{J}_{24} \end{bmatrix}^{-1} & \mathbf{0} \\ \begin{bmatrix} \mathbf{J}_{31} & \mathbf{J}_{32} \\ \mathbf{J}_{41} & \mathbf{J}_{42} \end{bmatrix}^{-1} \begin{bmatrix} \mathbf{J}_{33} & 0 \\ 0 & \mathbf{J}_{44} \end{bmatrix}^{-1} & \mathbf{0} \\ \mathbf{0}^{\mathsf{T}} & \sigma_v^2/4N \end{bmatrix} \tag{67}$$

The CRLB can be written as:

$$var(\theta^* - \widehat{\theta^*}) \geq$$

$$\begin{bmatrix} 2 & 0 & 0 & 0 & 0 \\ 0 & 2 & 0 & 0 & 0 \\ 0 & 0 & 2 & 0 & 0 \\ 0 & 0 & 0 & 2 & 0 \\ 0 & 0 & 0 & 0 & 1 \end{bmatrix} \begin{bmatrix} \begin{bmatrix} \mathbf{J}_{11} & 0 \\ 0 & \mathbf{J}_{22} \end{bmatrix}^{-1} \begin{bmatrix} \mathbf{J}_{13} & \mathbf{J}_{14} \\ \mathbf{J}_{23} & \mathbf{J}_{24} \end{bmatrix}^{-1} & \mathbf{0} \\ \begin{bmatrix} \mathbf{J}_{31} & \mathbf{J}_{32} \\ \mathbf{J}_{41} & \mathbf{J}_{42} \end{bmatrix}^{-1} \begin{bmatrix} \mathbf{J}_{33} & 0 \\ 0 & \mathbf{J}_{44} \end{bmatrix}^{-1} & \mathbf{0} \\ \mathbf{0}^{\mathsf{T}} & \sigma_v^2/4N \end{bmatrix} \tag{68}$$

For each sub-block, using the block matrix inverse identity we can rewrite the above inequality as:

$$var(\theta^* - \widehat{\theta^*}) \geq \begin{bmatrix} 2 & 0 & 0 & 0 & 0 \\ 0 & 2 & 0 & 0 & 0 \\ 0 & 0 & 2 & 0 & 0 \\ 0 & 0 & 0 & 2 & 0 \\ 0 & 0 & 0 & 0 & 1 \end{bmatrix} \times \begin{bmatrix} a_{11} & 0 & a_{13} & a_{14} & 0 \\ 0 & a_{22} & a_{23} & a_{24} & 0 \\ a_{31} & a_{32} & a_{33} & 0 & 0 \\ a_{41} & a_{42} & 0 & a_{44} & 0 \\ 0 & 0 & 0 & 0 & 1 \end{bmatrix} \tag{69}$$

where

$$\Delta_1 = \mathbf{J}_{13} - \mathbf{J}_{14}\mathbf{J}_{24}^{-1}\mathbf{J}_{23}, \tag{70}$$

$$\Delta_2 = \mathbf{J}_{31} - \mathbf{J}_{32}\mathbf{J}_{42}^{-1}\mathbf{J}_{41}, \tag{71}$$

$$a_{11} = \mathbf{J}_{11}^{-1}, \tag{72}$$

$$a_{13} = \Delta_1^{-1}, \tag{73}$$

$$a_{14} = -\Delta_1^{-1}\mathbf{J}_{14}\mathbf{J}_{24}^{-1}, \tag{74}$$

$$a_{22} = \mathbf{J}_{22}^{-1}, \tag{75}$$

$$a_{23} = -\mathbf{J}_{24}^{-1}\mathbf{J}_{23}\Delta_1^{-1}, \tag{76}$$

$$a_{24} = \mathbf{J}_{24}^{-1} + \mathbf{J}_{24}^{-1}\mathbf{J}_{23}\Delta_1^{-1}\mathbf{J}_{14}\mathbf{J}_{24}^{-1}, \tag{77}$$

$$a_{31} = \Delta_2^{-1}, \tag{78}$$

$$a_{32} = -\Delta_2^{-1}\mathbf{J}_{32}\mathbf{J}_{42}^{-1}, \tag{79}$$

$$a_{33} = \mathbf{J}_{33}^{-1}, \tag{80}$$

$$a_{41} = -\mathbf{J}_{42}^{-1}\mathbf{J}_{41}\Delta_2^{-1}, \tag{81}$$

$$a_{42} = \mathbf{J}_{42}^{-1} + \mathbf{J}_{42}^{-1}\mathbf{J}_{41}\Delta_2^{-1}\mathbf{J}_{32}\mathbf{J}_{42}^{-1}, \tag{82}$$

$$a_{44} = \mathbf{J}_{44}^{-1}. \tag{83}$$

Simplifying the above expression we get,

$$var(\theta^* - \hat{\theta}^*) > \sigma_v^2 \begin{bmatrix} \mathbf{J}(\mathrm{Re}\,\mathbf{h}) & 0 & 0 & 0 & 0 \\ 0 & \mathbf{J}(\mathrm{Im}\,\mathbf{h}) & 0 & 0 & 0 \\ 0 & 0 & \mathbf{J}(\mathrm{Re}\,x_0) & 0 & 0 \\ 0 & 0 & 0 & \mathbf{J}(\mathrm{Im}\,x_0) & 0 \\ 0 & 0 & 0 & 0 & \frac{1}{4N} \end{bmatrix} \tag{84}$$

where

$$\mathbf{J}(\mathrm{Re}\,\mathbf{h})^{-1} = 2\sigma_v^2 tr\Big(\sum_{n=0}^{N-1} E[\mathbf{s}_n \mathbf{s}_n^{\mathsf{H}}]^{-1}\Big) \tag{85}$$

$$\mathbf{J}(\mathrm{Im}\,\mathbf{h})^{-1} = 2\sum_{n=0}^{N-1} E[\mathbf{s}_n \mathbf{s}_n^{\mathsf{H}}]^{-1} \tag{86}$$

$$\mathbf{J}(\mathrm{Re}\,x_0)^{-1} = 2\sum_{n=0}^{N-1} \Big[E[(\mathbf{h}^{\mathsf{H}} \mathrm{Re}\,\mathbf{x}'_n)(\mathbf{h}^{\mathsf{H}} \mathrm{Re}\,\mathbf{x}'_n)^{\mathsf{H}}]\Big]^{-1} \tag{87}$$

$$\mathbf{J}(\mathrm{Im}\,x_0)^{-1} = 2\sum_{n=0}^{N-1} E[(\mathbf{h}^{\mathsf{H}} \mathrm{Im}\,\mathbf{x}'_n)(\mathbf{h}^{\mathsf{H}} \mathrm{Im}\,\mathbf{x}'_n)^{\mathsf{H}}]^{-1} \tag{88}$$

B. CRLB FOR DATA IN REAL DOMAIN

Here we show the derivation of the CRLB for data in real domain, denoted as CRLB(Re θ). The first and second order partial derivatives are:

$$\text{(a)}\ \frac{\partial \ell(\mathbf{y}|\theta)}{\partial \mathbf{h}} = \frac{1}{\sigma_v^2}[\sum_{n=1}^{N} y_n \mathbf{s}_n - \mathbf{h}^{\mathsf{T}} \sum_{n=1}^{N} \mathbf{s}_n \mathbf{s}_n^T]$$

$$\text{(b)}\ \frac{\partial \ell(\mathbf{y}|\theta)}{\partial x_0} = \frac{1}{\sigma_v^2}[\sum_{n=0}^{N-1} (y_n - \mathbf{h}^{\mathsf{T}}\mathbf{s}_n)\mathbf{h}^{\mathsf{T}}\mathbf{x}'_n]$$

$$\text{(c)}\ \frac{\partial \ell(\mathbf{y}|\theta)}{\partial \sigma_v} = -\frac{N}{\sigma_v} + \frac{1}{\sigma_v^3}\sum_{n=0}^{N-1}(y_n - \mathbf{h}^{\mathsf{T}}\mathbf{s}_n)^2$$

$$\text{(d)}\ \frac{\partial^2 \ell(\mathbf{y}|\theta)}{\partial \sigma_v^2} = \frac{N}{\sigma_v^2} - \frac{3}{\sigma_v^4}\sum_{n=0}^{N-1} v_n^2 = -\frac{2N}{\sigma_v^2}$$

$$\text{(e)}\ \frac{\partial^2 \ell(\mathbf{y}|\theta)}{\partial \mathbf{h}^2} = -\frac{1}{2\sigma_v^2}\sum_{n=0}^{N-1} \mathbf{s}_n \mathbf{s}_n^{\mathsf{T}}$$

$$\text{(f)}\ \frac{\partial^2 \ell(\mathbf{y}|\theta)}{\partial x_0^2} = \frac{1}{\sigma_v^2}\sum_{n=0}^{N-1} v_n \mathbf{h}^{\mathsf{T}}\mathbf{x}''_n - (\mathbf{h}^{\mathsf{T}}\mathbf{x}'_n)^2$$

$$\text{(g)}\ \frac{\partial^2 \ell(\mathbf{y}|\theta)}{\partial x_0 \partial \mathbf{h}} = \frac{1}{\sigma_v^2}\sum_{n=0}^{N-1}(v_n \mathbf{x}'_n - \mathbf{s}_n[\mathbf{x}'_n]^{\mathsf{T}}\mathbf{h})$$

$$\text{(h)}\ \frac{\partial^2 \ell(\mathbf{y}|\theta)}{\partial \mathbf{h} \partial x_0} = \frac{1}{\sigma_v^2}\sum_{n=0}^{N-1}(v_n \mathbf{x}'_n - \mathbf{h}^{\mathsf{T}}\mathbf{s}_n[\mathbf{x}'_n]),$$

where $\sum_{n=0}^{N-1} v_n^2 = N\sigma_v^2$

The FIM of the inverse map becomes,

$$\mathbf{J}(\theta) = -E\begin{bmatrix} \frac{\partial^2 \ell(\mathbf{y}|\theta)}{\partial \mathbf{h}^2} & \frac{\partial^2 \ell(\mathbf{y}|\theta)}{\partial \mathbf{h} \partial x_0} & \frac{\partial^2 \ell(\mathbf{y}|\theta)}{\partial \mathbf{h} \partial \sigma_v} \\ \frac{\partial^2 \ell(\mathbf{y}|\theta)}{\partial x_0 \partial \mathbf{h}} & \frac{\partial^2 \ell(\mathbf{y}|\theta)}{\partial x_0^2} & \frac{\partial^2 \ell(\mathbf{y}|\theta)}{\partial x_0 \partial \sigma_v} \\ \frac{\partial^2 \ell(\mathbf{y}|\theta)}{\partial \sigma_v \partial \mathbf{h}} & \frac{\partial^2 \ell(\mathbf{y}|\theta)}{\partial \sigma_v \partial x_0} & \frac{\partial^2 \ell(\mathbf{y}|\theta)}{\partial \sigma_v^2} \end{bmatrix}$$
$$= \frac{1}{\sigma_v^2}\begin{bmatrix} \sum_{n=0}^{N-1} E[\mathbf{s}_n \mathbf{s}_n^{\mathsf{T}}] & \sum_{n=0}^{N-1} E[\mathbf{s}_n[\mathbf{x}'_n]^{\mathsf{T}}\mathbf{h}] & 0 \\ \sum_{n=0}^{N-1} E[\mathbf{h}^{\mathsf{T}}\mathbf{s}_n \mathbf{x}'_n] & \sum_{n=0}^{N-1} E[(\mathbf{h}^{\mathsf{T}}\mathbf{x}'_n)^2] & 0 \\ 0 & 0 & 2N \end{bmatrix}. \quad (89)$$

For ease of representation, let

$$J_{11} = \frac{1}{\sigma_v^2}\sum_{n=0}^{N-1} E\left[\mathbf{s}_n \mathbf{s}_n^{\mathsf{T}}\right], \quad (90)$$

$$J_{12} = \frac{1}{\sigma_v^2}\sum_{n=0}^{N-1} E[\mathbf{s}_n[\mathbf{x}'_n]^{\mathsf{T}}\mathbf{h}], \quad (91)$$

$$J_{21} = \frac{1}{\sigma_v^2}\sum_{n=0}^{N-1} E[\mathbf{h}^{\mathsf{T}}\mathbf{s}_n \mathbf{x}'_n], \quad (92)$$

$$J_{22} = \frac{1}{\sigma_v^2}\sum_{n=0}^{N-1} E[(\mathbf{h}^{\mathsf{T}}\mathbf{x}'_n)^2] \quad (93)$$

The CRLB can then be written as:

$$\mathbf{J}^{-1}(\theta) = \sigma_v^2\begin{bmatrix} J_{11} & J_{12} & 0 \\ J_{21} & J_{22} & 0 \\ 0 & 0 & 2N \end{bmatrix}^{-1} \quad (94)$$

$$= \sigma_v^2\begin{bmatrix} \begin{bmatrix} J_{11} & J_{12} \\ J_{21} & J_{22} \end{bmatrix}^{-1} & \mathbf{0} \\ \mathbf{0}^T & 1/2N \end{bmatrix} \quad (95)$$

Using block matrix inverse identity, we can rewrite the above inequality as,

$$= \sigma_v^2\begin{bmatrix} \Delta_1^{-1} & -\Delta_1^{-1}J_{12}J_{22}^{-1} & 0 \\ -J_{22}^{-1}J_{21}\Delta_1^{-1} & J_{22}^{-1} + J_{22}^{-1}J_{21}\Delta_1^{-1}J_{12}J_{22}^{-1} & 0 \\ 0 & 0 & 1/2N \end{bmatrix} \quad (96)$$

where $\mathbf{0} = [0, 0]^{\mathsf{T}}$ and $\Delta_1 = J_{11} - J_{12}J_{22}^{-1}J_{21}$. We are interested in the estimation error variance of $\mathbf{h}$, i.e., $E[\Delta\mathbf{h}^{\mathsf{T}}\Delta\mathbf{h}]$, where $\Delta\mathbf{h} = \hat{\mathbf{h}} - \mathbf{h}$ and $\hat{\mathbf{h}}$ is the estimate. From (96), we have

$$E[\Delta\mathbf{h}^{\mathsf{T}}\Delta\mathbf{h}] \geq tr(\Delta_1^{-1}) = \sigma_v^2 tr([J_{11} - J_{12}J_{22}^{-1}J_{21}]^{-1}) \quad (97)$$

By chaos representation of the RS we are exploiting the Lyapunov Exponents (LE) of the chaos map. We believe that by exploiting this unique characteristic of chaos, system identification performance can be improved. Moreover, the chaos representation of random signal allows the chaotic map to behave as the source of information with entropy depending on the LE. The LE depends on the number of piecewise linear segments as explained in this section. From the inverse mapping function we have the derivative as:

$$x'_{n+1} = f_{s_n}^{-1'}(x_{n+1}) = \{p_1, p_2, \ldots, p_m\} \quad (98)$$

and the square of the gradient x'_n is independent of x. The first order derivative of f is

$$f'(x) = \frac{1}{p_1}, 0 < x < p_1,$$
$$\cdots$$
$$= \frac{1}{p_m}, 0 < x < p_m \quad (99)$$

and the square of the gradient $f'(x)$ is independent of x. Since, f is equivalent to σ [49], LE does not change and is expressed as [50]

$$\lambda = \sum_{i=1}^{m} p_i \log(f') \quad (100)$$

where $p \in (0, 1)$. For example, when $m = 2$ the LE in (100) evaluates to $\lambda = (1-p)\ln(2/(1-p)) + p\ln(1/p)$ where p denotes the probability of occurrence of symbol 0. As a result, employing the LE which is unique to chaos is certainly advantageous in system identification. Since, the PWL chaotic map is a 1D nonlinear dynamical system, it has only one positive λ. Assuming that the process is ergodic, the time average is equivalent to the phase-space average, it follows that when $N \to \infty$, we have

$$E\left[\left(\frac{\partial x_N}{\partial x_0}\right)^2\right] = \left\langle \left(\frac{\partial x_N}{\partial x_0}\right)^2 \right\rangle = \exp(2(N)\lambda) \quad (101)$$

where $\langle . \rangle$ represents the phase space average. As $\lambda > 0$, $\exp(2(N)\lambda) >> \exp(2\lambda)$ and $\exp(2(N)\lambda)$ increases exponentially, we have $E\left[\sum_{n=0}^{N-1}\left(\frac{\partial x_n}{\partial x_0}\right)^2\right] \rightarrow \infty$ as $N \rightarrow \infty$. Therefore,

$$J_{22}^{-1} = E[\textstyle\sum_{n=0}^{N-1} \mathbf{h}^{\mathsf{T}}[\mathbf{x}'_n]^2] \rightarrow 0 \tag{102}$$

We have the CRLB of the proposed method as:

$$\mathbf{J}^{-1}(\mathbf{h}) = \sigma_v^2 tr([J_{11}]^{-1}) = \sigma_v^2 tr\left(\left[E\left[\sum_{n=0}^{N-1} \mathbf{s}_n \mathbf{s}_n^{\mathsf{T}}\right]\right]^{-1}\right). \tag{103}$$

and approaches the CRLB asymptotically for large N. The estimates are efficient and the MSE converges to the theoretic CRLB as N $\rightarrow \infty$.

REFERENCES

[1] H. Leung, *Chaotic signal Processing*, vol. 136. Philadelphia, PA, USA: SIAM, 2013.

[2] H. Leung, "System identification using chaos with application to equalization of a chaotic modulation system," *IEEE Trans. Circuits Syst. I, Fundam. Theory Appl.*, vol. 45, no. 3, pp. 314–320, Mar. 1998.

[3] Z. Zhu and H. Leung, "Identification of linear systems driven by chaotic signals using nonlinear prediction," *IEEE Trans. Circuits Syst. I, Fundam. Theory Appl.*, vol. 49, no. 2, pp. 170–180, Feb. 2002.

[4] W. Hu, L. Wang, G. Cai, and G. Chen, "Non-coherent capacity of M-ary DCSK modulation system over multipath Rayleigh fading channels," *IEEE Access*, vol. 5, pp. 956–966, 2017.

[5] P. Chen, Y. Fang, G. Han, and G. Chen, "An efficient transmission scheme for dcsk cooperative communication over multipath fading channels," *IEEE Access*, vol. 4, pp. 6364–6373, 2016.

[6] G. Kaddoum, "Wireless chaos-based communication systems: A comprehensive survey," *IEEE Access*, vol. 4, pp. 2621–2648, May 2016.

[7] H. Leung, S. Shanmugam, N. Xie, and S. Wang, "An ergodic approach for chaotic signal estimation at low SNR with application to ultra-wideband communication," *IEEE Trans. Signal Process.*, vol. 54, no. 3, pp. 1091–1103, Mar. 2006.

[8] B. B. Ferreira, A. S. de Paula, and M. A. Savi, "Chaos control applied to heart rhythm dynamics," *Chaos, Solitons Fractals*, vol. 44, no. 8, pp. 587–599, 2011.

[9] M. E. Cohen, D. L. Hudson, and P. C. Deedwania, "Applying continuous chaotic modeling to cardiac signal analysis," *IEEE Eng. Med. Biol. Mag.*, vol. 15, no. 5, pp. 97–102, Sep./Oct. 1996.

[10] C. Xiu, J. Hou, Y. Zang, G. Xu, and C. Liu, "Synchronous control of hysteretic creep chaotic neural network," *IEEE Access*, vol. 4, pp. 8617–8624, Dec. 2016.

[11] H. Leung and T. Lo, "Chaotic radar signal processing over the sea," *IEEE J. Ocean. Eng.*, vol. 18, no. 3, pp. 287–295, Jul. 1993.

[12] B. C. Flores, E. A. Solis, and G. Thomas, "Assessment of chaos-based fm signals for range-Doppler imaging," *IEE Proc.-Radar, Sonar Navigat.*, vol. 150, no. 4, p. 313, Aug. 2003.

[13] C. Ellegaard, K. Schaadt, and P. Bertelsen, "Acoustic chaos," in *Quantum Chaos Y2K*. Singapore: World Scientific, 2001, pp. 223–230.

[14] Y. Zhang, L. Y. Zhang, J. Zhou, L. Liu, F. Chen, and X. He, "A review of compressive sensing in information security field," *IEEE Access*, vol. 4, pp. 2507–2519, 2016.

[15] Y. Nakamura and A. Sekiguchi, "The chaotic mobile robot," *IEEE Trans. Robot. Autom.*, vol. 17, no. 6, pp. 898–904, Dec. 2001.

[16] S. Mukhopadhyay and H. Leung, "Dynamical systems approach for predator-prey robot behavior control via symbolic dynamics based communication," in *Encyclopedia of Information Science and Technology*, 3rd ed. Hershey, PA, USA: IGI Global, 2015, pp. 6621–6632.

[17] N. Xie and H. Leung, "Blind identification of autoregressive system using chaos," *IEEE Trans. Circuits Syst. I, Reg. Papers*, vol. 52, no. 9, pp. 1953–1964, Sep. 2005.

[18] A. Kurian and H. Leung, "System identification using chaos," in *Chaotic Signal Processing*, H. Leung, Ed. Philadelphia, PA, USA: SIAM, 2014, ch. 5.

[19] S. Kay and V. Nagesha, "Methods for chaotic signal estimation," *IEEE Trans. Signal Process.*, vol. 43, no. 8, pp. 2013–2016, Aug. 1995.

[20] L. Cong, W. Xiaofu, and S. Songgeng, "A general efficient method for chaotic signal estimation," *IEEE Trans. Signal Process.*, vol. 47, no. 5, pp. 1424–1428, May 1999.

[21] H. C. Papadopoulos and G. W. Wornell, "Maximum-likelihood estimation of a class of chaotic signals," *IEEE Trans. Inf. Theory*, vol. 41, no. 1, pp. 312–317, Jan. 1995.

[22] C. Pantaleón, D. Luengo, and I. Santamaría, "Piecewise-linear maps," *IEEE Signal Process. Lett.*, vol. 7, no. 8, pp. 235–237, Aug. 2000.

[23] S. Wang, P. C. Yip, and H. Leung, "Estimating initial conditions of noisy chaotic signals generated by piecewise linear Markov maps using itineraries," *IEEE Trans. Signal Process.*, vol. 47, no. 12, pp. 3289–3302, Dec. 1999.

[24] D. Luengo, I. Santamaría, and L. Vielva, "Asymptotically optimal maximum-likelihood estimation of a class of chaotic signals using the Viterbi algorithm," in *Proc. IEEE 13th Eur. Signal Process. Conf.*, Sep. 2005, pp. 1–4.

[25] M. Ciftci and D. B. Williams, "Optimal estimation and sequential channel equalization algorithms for chaotic communications systems," *EURASIP J. Appl. Signal Process.*, vol. 2001, no. 1, pp. 249–256, 2001.

[26] D. Luengo and I. Santamaría, "Secure communications using OFDM with chaotic modulation in the subcarriers," in *Proc. IEEE 61st Veh. Technol. Conf. (VTC-Spring)*, vol. 2. May/Jun. 2005, pp. 1022–1026.

[27] G. Kaddoum, F. Gagnon, and D. Couillard, "An enhanced spectral efficiency chaos-based symbolic dynamics transceiver design," in *Proc. 6th Int. Conf. Signal Process. Commun. Syst.*, Dec. 2012, pp. 1–6.

[28] G. Kaddoum, G. Gagnon, and F. Gagnon, "Spread spectrum communication system with sequence synchronization unit using chaotic symbolic dynamics modulation," *Int. J. Bifurcation Chaos*, vol. 23, no. 2, p. 1350019, 2013.

[29] R. Candido, D. C. Soriano, M. T. M. Silva, and M. Eisencraft, "Do chaos-based communication systems really transmit chaotic signals?" *Signal Process.*, vol. 108, pp. 412–420, Mar. 2015.

[30] H.-P. Ren, M. S. Baptista, and C. Grebogi, "Wireless communication with chaos," *Phys. Rev. Lett.*, vol. 110, no. 18, p. 184101, Apr. 2013.

[31] C. Vural and G. Çetinel, "Blind equalization of single-input single-output fir channels for chaotic communication systems," *Digit. Signal Process.*, vol. 20, no. 1, pp. 201–211, 2010.

[32] M. Xu, Y. Song, and L. Liu, "Adaptive blind equalization for chaotic communication systems using particle filtering," in *Proc. IEEE 8th Int. Conf. Signal Process.*, vol. 3. Nov. 2006.

[33] X. Xu, J. Guo, and H. Leung, "Blind equalization for power-line communications using chaos," *IEEE Trans. Power Del.*, vol. 29, no. 3, pp. 1103–1110, Jun. 2014.

[34] Z. Zhu and H. Leung, "Adaptive blind equalization for chaotic communication systems using extended-Kalman filter," *IEEE Trans. Circuits Syst. I, Fundam. Theory Appl.*, vol. 48, no. 8, pp. 979–989, Aug. 2001.

[35] G. Rigatos, "A chaotic communication system of improved performance based on the derivative-free nonlinear Kalman filter," *Int. J. Syst. Sci.*, vol. 47, no. 9, pp. 2152–2168, 2016.

[36] V. Venkatasubramanian and H. Leung, "An EM based method for semi blind identification of linear systems driven by chaotic signals," in *Proc. IEEE Conf. Cybern. Intell. Syst.*, vol. 1. Dec. 2004, pp. 554–557.

[37] X. Liu, T. Sabbir, and H. Leung, "Cognitive identification of systems using nonlinear dynamics," in *Proc. IEEE 13th Int. Conf. Cognit. Inform. Cognit. Comput.*, Aug. 2014, pp. 61–66.

[38] M. W. Hirsch, S. Smale, and R. L. Devaney, *Differential Equations, Dynamical Systems, and an Introduction to Chaos*. San Francisco, CA, USA: Academic, 2012.

[39] R. Gilmore and M. Lefranc, "Discrete dynamical systems: Maps," in *The Topology of Chaos: Alice in Stretch and Squeezeland*. New York, NY, USA: Wiley,

[40] V. Venkatasubramanian and H. Leung, "Chaos based semi-blind system identification using an EM-UKS estimator," in *Proc. IEEE Int. Conf. Syst., Man Cybern.*, vol. 3. Oct. 2005, pp. 2873–2878.

[41] F. Girosi and T. Poggio, "Networks and the best approximation property," *Biol. Cybern.*, vol. 63, no. 3, pp. 169–176, 1990.

[42] T. L. Carroll and F. J. Rachford, "Chaotic sequences for noisy environments," *Chaos, Interdiscipl. J. Nonlinear Sci.*, vol. 26, no. 10, p. 103104, 2016.

[43] S. M. Kay, *Fundamentals of Statistical Signal Processing*. Englewood Cliffs, NJ, USA: Prentice-Hall, 1993.

[44] P. Stoica and N. Arye, "MUSIC, maximum likelihood, and Cramer–Rao bound," *IEEE Trans. Acoust., Speech Signal Process.*, vol. 37, no. 5, pp. 720–741, May 1989.

[45] S. Särkkä, "Unscented Rauch–Tung–Striebel smoother," *IEEE Trans. Autom. Control*, vol. 53, no. 3, pp. 845–849, Apr. 2008.

[46] C.-Y. Chi, C.-Y. Chen, C.-H. Chen, and C.-C. Feng, "Batch processing algorithms for blind equalization using higher-order statistics," *IEEE Signal Process. Mag.*, vol. 20, no. 1, pp. 25–49, Jan. 2003.

[47] S. Abrar and A. K. Nandi, "Blind equalization of square-QAM signals: A multimodulus approach," *IEEE Trans. Commun.*, vol. 58, no. 6, pp. 1674–1685, Jul. 2010.

[48] G. Giunta and F. Benedetto, "A signal processing algorithm for multi-constant modulus equalization," in *Proc. IEEE 36th Int. Conf. Telecommun. Signal Process. (TSP)*, Jul. 2013, pp. 52–56.

[49] J. Juang and S.-F. Shieh, "Piecewise linear maps, Liapunov exponents and entropy," *J. Math. Anal. Appl.*, vol. 338, no. 1, pp. 358–364, 2008.

[50] K. Feltekh, D. Fournier-Prunaret, and S. Belghith, "Analytical expressions for power spectral density issued from one-dimensional continuous piecewise linear maps with three slopes," *Signal Process.*, vol. 94, pp. 149–157, Jan. 2014.

SUMONA MUKHOPADHYAY received the Ph.D. degree in electrical and computer engineering from the University of Calgary, Calgary, AB, Canada, in 2018. Her research interests include signal processing and machine learning.

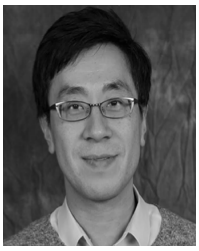

HENRY LEUNG (F'15) was with the Department of National Defence of Canada as a Defence Scientist. He is currently a Professor of the Department of Electrical and Computer Engineering, University of Calgary. His current research interests include information fusion, machine learning, nonlinear dynamics, robotics, and signal and image processing. He is a fellow of SPIE. He is an Associate Editor of *IEEE Circuits and Systems Magazine*. He is a Topic Editor on Robotic Sensors of the *International Journal of Advanced Robotic Systems*. He is an Editor of the Springer book series on Information Fusion and Data Science.